cytokine signaling (SOCS) (Yoshimura *et al.* 2005). SOCS proteins are induced in response to cytokine signaling, and further hinder signaling by blocking the Jak-Stat pathway. Members of the SOCS family form a negative feedback loop with key actions involving inhibition of the Jak-Stat signaling cascade. There are eight members of the SOCS protein family: the cytokine-inducible SH2 domain-containing protein (CIS) and SOCS1 through SOCS7. All eight members contain an N-terminal region of varying length and sequence, a central SH2 domain, and a conserved C-terminal SOCS box. One of the best characterized members is SOCS3.

SOCS3 was initially found to be induced by erythropoietin and granulocyte-macrophage colony stimulating factor in certain hematopoietic cells. It is involved in erythropoiesis regulation (Starr *et al.* 1997). Increasing evidence suggests that SOCS3 plays a negative regulatory role in Stat3. SOCS3 has been shown to interact with gp130 and Jak, and this interaction results in relatively specific inhibition of gp130 signaling (Nicholson *et al.* 2000; Schmitz *et al.* 2000). Transient expression of SOCS3 inhibits LIF-induced Stat3 reporter gene activation (Rakesh and Agrawal 2005). Phosphorylation of Stat3 is prolonged in mouse SOCS3-deficient macrophages after stimulation with IL-6, indicating that SOCS3 specifically affects signaling mediated by IL-6 and gp130 (Lang *et al.* 2003).

As Stat3 plays essential roles in the differentiation of neural stem cells, we speculated that SOCS3 also regulates neural stem cell fate. To confirm this, we applied an adenoviral vector expressing SOCS3 and investigated the direct effects of SOCS3 on neural stem cells.

In addition, Notch family members (notch1–3) and inhibitory bHLH transcription factors (hes1 and 5, id1–3) play important roles in proliferation, cell lineage determination and cell differentiation of neural stem cells (Lasky and Wu 2005). bHLH determination factor (mash1) and bHLH differentiation factors (neuroD1 and neuroD2) play important roles in initiating neurogenesis and mediating terminal neuronal differentiation, respectively (Ross *et al.* 2003). Conversely, Sox9 plays an important role in causing neural stem cells to switch from neurogenesis to gliogenesis (Stolt *et al.* 2003). For these reasons, we also investigated the effect of SOCS3 on mRNA expression of these genes.

The results showed that overexpression of SOCS3 promoted neurogenesis and inhibited astrogliogenesis in neural stem cells. Our results also showed that SOCS3 promoted maintenance of neural stem cells, probably through up-regulation of notch1.

Materials and methods

All experiments were conducted according to the Guidelines for Animal Experimentation at Ehime University Graduate School of Medicine and were approved by our institutional Ethics Committee.

Adenoviral vectors

A recombinant adenovirus expressing human SOCS3 was constructed as described previously (Shouda *et al.* 2001). Human SOCS3 DNA was excised and the resultant expression units were inserted at the SwaI site of the cosmid vector, pAxCAwt (RBD:1678, Bio Resource Center, Riken, Wako, Japan). Cosmid DNA was cotransfected with the DNA-terminal protein complex into human kidney 293 cells to generate a recombinant virus (Ad.SOCS3). An adenovirus expressing β-galactosidase with nuclear signaling (Ad.Lz) was provided by Dr Izumu Saito (University of Tokyo, Tokyo, Japan). Each recombinant virus was propagated in 293 cells and purified by CsCl step-gradient ultracentrifugation. Viral titers were determined using the modified end-point cytopathic effect assay (Kanegae *et al.* 1994).

Neurosphere generation and maintenance

Neural stem cells were isolated from rat embryos (Wistar rats, day 17–18). The embryonic rat brain was cleared of meninges, and striatal tissue from both hemispheres was dissected using fine forceps. The tissue was mechanically triturated, and cell suspensions were seeded in 9-cm dishes (Sumilon MS13900, Sumitoko Bakelite Co. Ltd, Tokyo, Japan) in growth medium composed of Dulbecco's modified Eagle's medium (DMEM; Sigma Chemical Co., St. Louis, MO, USA) containing 0.2 mg/mL bovine serum albumin (BSA; A-7638, Sigma, St. Louis, MO), 10 mM HEPES, 4.5 mg/mL glucose, 5 μg/mL insulin, 5 nM sodium selenite, 5 μg/mL transferrin and 40 ng/mL human recombinant epidermal growth factor (EGF, Upstate Biotechnology, Lake Placid, NY). Antibiotics and antimycotics (penicillin 100 units/mL; streptomycin 100 μg/mL; amphotericin B 0.25 μg/mL, Sigma) were also included. Neural stem cells were grown as neurospheres.

Viral infection and differentiation of neuronal progenitor cells

Five days after seeding, neurospheres were dissociated mechanically and neural stem cells were exposed to adenoviral vector expressing SOCS3 or Lz [multiplicity of infection (moi) = 10] for 1 h in the same growth medium. Cells were then seeded at a density of 5×10^5/mL on poly-L-lysine-coated 24-well dishes in the differentiating medium (Neurobasal medium; Invitrogen, Gaithersburg, MD, USA) containing B27 supplement (Invitrogen), all-*trans*-retinoic acid (10^{-7} M, Sigma), 2 mM L-glutamine and antibiotics (penicillin 50 units/mL, streptomycin 50 μg/mL). Some were incubated in the differentiating medium in the presence of AG490 (10 μM, Calbiochem, La Jolla, CA, USA). For the positive control, infected stem cells were incubated in the differentiating medium. One day later, some stem cells were treated with recombinant mouse LIF (30 ng/mL, Chemicon, Temecula, CA, USA) and bFGF (10 ng/mL, Genzyme Techne, Minneapolis, MN, USA). Treatment with LIF and bFGF has been reported to activate Stat3 and promote astrogliogenesis in neural stem cells (Molne *et al.* 2000).

Luciferase promoter assay

The constructs of the Stat3 reporter plasmids have been described elsewhere (Nakajima *et al.* 1996). In brief, the Stat3 reporter plasmid contains four copies of the acute-phase response element (APRE) in front of the minimal junB promoter linked to the luciferase gene. The response element was the APRE of the rat alpha 2-macroglobulin gene, 5′-GCGCCTTCTGGGAAGATCCTTACG-

© 2006 The Authors
Journal Compilation © 2006 International Society for Neurochemistry,

GGAATTCAG-3′. The cultured neurospheres were washed once in phosphate-buffered saline (PBS), and resuspended in the specified electroporation buffer to a final concentration of 1×10^7 cells/mL. Then, 10 μg Stat3 reporter plasmid and 4 μg pRL-TK (Promega, Madison, WI, USA) internal control plasmid DNA were mixed with 0.1 mL cell suspension, transferred to a 2.0-mm electroporation cuvette, and electroporated with an Amaxa Nucleofector apparatus (Amaxa, Cologne, Germany). The transfected stem cells were then exposed to adenoviral vector expressing SOCS3 or Lz (10 moi) for 1 h in the differentiating medium. One day after electroporation, some stem cells were treated with LIF (30 ng/mL) and bFGF (10 ng/mL). Two days after electroporation, the activity of firefly luciferase from Stat3 promoter-luciferase plasmid and renilla luciferase from pRL-TK plasmid in the cell extracts was evaluated using a Dual-luciferase assay kit (Promega) with a luminometer (TD-20/20, Turner Biosystems, Sunnyvale, CA, USA). Relative firefly luciferase activity was calculated by normalizing the transfection efficiency according to the renilla luciferase activity.

Immunoblot analysis

Cells were solubilized in Laemmli's lysis buffer containing 2% sodium dodecyl sulfate (SDS). The suspension was resolved by electrophoresis, transferred to nitrocellulose sheets and immunoblotted using a rabbit polyclonal antibody against GFAP (G9269, Sigma) protein or mouse monoclonal antibodies against beta-actin (A5441, Sigma), Stat3 (sc-8019, Santa Cruz Biotechnology, Santa Cruz, CA, USA), pStat3 (Tyr705 phosphorylated Stat3, sc-8059, Santa Cruz Biotechnology), SOCS3 (sc-9023, Santa Cruz Biotechnology), microtubule-associated protein 2 (MAP2, SMI 52, Sternberger Monoclonals Inc., Lutherville, MD, USA), Tuj1 (MMS-435P, Covance Research, Berkeley, CA, USA) and Nestin (MAB353, Chemicon, Temecula, CA, USA) proteins. The second antibodies were alkaline phosphatase-conjugated anti-rabbit IgG for the rabbit polyclonal antibody or alkaline phosphatase-conjugated anti-mouse IgG for the mouse monoclonal antibodies. The density of immunoreactive bands was measured using NIH image software (National Institutes of Health, Bethesda, MD, USA) as described previously (Gu *et al.* 2003).

Immunocytochemistry

Cells were washed with PBS and fixed for 30 min with 4% paraformaldehyde in 0.1 M phosphate buffer (pH 7.4). After three washes with PBS, the samples were incubated with 10% normal goat serum dissolved in PBS. Either a primary mouse monoclonal antibody against MAP2 (Sternberger Monoclonals) and GFAP (G3893, Sigma) or a rabbit polyclonal antibody against β-galactosidase (AB1211, Chemicon), SOCS3 (SC-9023, Santa Cruz Biotechnology) and GFAP (Progen, Heidelberg, Germany) was incubated with the samples at 4°C overnight. The samples were washed three times with PBS, incubated with rhodamine-conjugated goat anti-mouse IgG (ICN, Irvine, CA, USA) or with fluorescein-5-isothiocyanate (FITC)-conjugated goat anti-rabbit IgG (ICN) for 30 min at room temperature, washed three times with PBS, and mounted in Vectashield (Vector Laboratory, Burlingame, CA, USA).

Reverse transcription polymerase chain reaction (RT-PCR)

Cells were washed with PBS, and total RNA was extracted using Isogen (Nippon Gene, Tokyo, Japan). Total RNA was digested with DNase, and then single stranded cDNA was obtained using oligo dT primers and Moloney murine leukemia virus reverse transcriptase (Invitrogen). The PCR was carried out using Ex Taq polymerase (Takara, Tokyo, Japan). The synthesized cDNA was amplified under the following conditions: initial denaturation at 94°C for 5 min; denaturation at 94°C for 1 min; annealing at 55–57°C for 1.5 min; and extension at 72°C for 1.5 min for 20–38 cycles. The PCR conditions were optimized by varying the annealing temperature and cycle number to determine the linear amplification range. Amplification products were identified by size and confirmed by DNA sequencing. Table 1 summarizes the primer sequences, annealing temperature, cycle number and PCR product size for each pair of probes. The PCR products separated on 3% agarose gels were visualized by staining with ethidium bromide and semiquantified using an NIH image analysis system (National Institutes of Health).

Statistical analysis

Data are presented as mean ± SD. Unless indicated, differences were evaluated using the Mann–Whitney *U*-test for statistical significance. A *p*-value of less than 0.05 was considered statistically significant.

Results

Suppression of Stat3 cell signaling machinery after overexpression of SOCS3

We initially examined whether neural stem cells expressed Stat3 and SOCS3 protein after infection with adenoviral vectors. One day or 3 days after viral infection, cells were homogenized in lysis buffer and immunoblotted with antibody against β-actin, Stat3, Tyr-705 phosphorylated Stat3 (pStat3) or SOCS3. One day and 3 days after infection (Figs 1a and e), strong SOCS3 expression was evident in Ad.SOCS3-infected cells but not in Ad.Lz-infected cells. Stat3 protein was weakly expressed in both Ad.Lz- and Ad.SOCS3-infected cells. Moreover, pStat3 was weakly activated in Ad.Lz-infected cells, and no activation of pStat3 was evident in Ad.SOCS3-infected cells. These data suggest that SOCS3 could suppress Stat3 cell signaling in neural stem cells.

To confirm whether Ad.SOCS3 could actually inhibit Stat3 function in neural stem cells, we introduced minimal junB reporter constructs with or without four copies of APRE into Ad.SOCS3-infected or Ad.Lz-infected stem cells in the presence and absence of LIF (30 ng/mL) and bFGF (10 ng/mL). Treatment with LIF and bFGF has been reported to activate Stat3 and promote astrogliogenesis in neural stem cells (Molne *et al.* 2000). A dual luciferase assay was carried out 1 day after the treatment. Relative luciferase activity in Ad.SOCS3-infected cells was significantly lower than that in Ad.Lz-infected cells after transfection of Stat3 reporter plasmid (minimal junB promoter with four copies of APRE) (Fig. 2a). In addition, relative luciferase activity in the

© 2006 The Authors

Table 1 Sequences, annealing temperatures (Tm, °C), cycle numbers, PCR product sizes (bp) for each pair of probes

Primer	Sequence (5′-3′)	Annealing Tm (°C)	Cycle	Product size (bp)
β-actin F	AGAAGAGCTATGAGCTGCCTGACG	55	20	312
β-actin R	TACTTGCGCTCAGGAGGAGCAATG			
Notch1 F	TGTGACAGCCAGTGCAACTC	57	32	547
Notch1 R	TGGCGCTCTGGAAGCATTGC			
Notch2 F	GCCGTCAGACTGGAGACTTC	57	32	640
Notch2 R	GCGTAGCCCTTCAGACACTC			
Notch3 F	AGTCACTGCGAACAGGAGGT	57	32	514
Notch3 R	AGGGGAACAGAGCAGTCTGA			
Hes1 F	CGAGCGTGTTGGGGAAGTA	57	35	101
Hes1 R	AGTGCGCACCTCGGTGTTA			
Hes5 F	GATGCTCAGTCCCAAGGAGA	57	35	336
Hes5 R	CGCTGGAAGTGGTAAAGCAG			
Id1 F	GATCATGAAGGTCGCCAGTAG	57	32	218
Id1 R	GCTCCTTGAGGCGTGAGTAG			
Id2 F	CTCCAAGCTCAAGGAACTGG	57	32	207
Id2 R	ATGCTGATGTCCGTGTTCAG			
Id3 F	CTGTCGGAACGTAGCCTAGC	57	32	177
Id3 R	GTCTATGACACGCTGCAGGA			
Mash1 F	AAGTCAGCGGCCAAGCAGGTCAAG	57	32	245
Mash1 R	CGCAGCGTCTCCACCTTGCTCATCT			
NeuroD1 F	CCAGACCTCGTCTCCTTTGTA	57	35	314
NeuroD1 R	GGGCTGGTGCAATCAGTTAG			
NeuroD2 F	GGCCGAAGAAACGCAAGATG	57	33	265
NeuroD2 R	GCACAGAGTCTGCACGTAGG			
Sox9 F	AAGAAGGAGAGCGAGGAAGATA	56	33	216
Sox9 R	GTTGTGCAGATGCGGGTACT			

positive control cells (Ad.Lz + LIF + bFGF-infected cells) was markedly higher (approximately 5.5-fold) than that in Ad.Lz-infected cells. Furthermore, this LIF-induced transcriptional activation was inhibited completely by overexpression of SOCS3 (Fig. 2a).

On the other hand, no significant differences of relative luciferase activity could be detected after transfection of the control reporter plasmid (minimal junB promoter without APRE) among the groups (Fig. 2b). These results support the notion that SOCS3 can act as a negative regulator of Stat3 cell signaling in neural stem cells.

Promotion of neurogenesis and inhibition of astrogliogenesis by overexpression of SOCS3

We next examined whether overexpression of SOCS3 could modulate the differentiation of neural stem cells. One or 3 days after infection, cells were homogenized in lysis buffer and immunoblotted with an antibody against Nestin – a marker for neural stem cells, GFAP – a specific marker of astrocytes, and MAP2 – a specific marker for neurons.

Densitometric analysis revealed that 1 day after infection, levels of GFAP, Nestin and MAP2 proteins did not differ between cells infected with Ad.Lz and Ad.SOCS3 (Figs 1a–d). However, 3 days after infection, the level of GFAP protein in Ad.SOCS3-infected cells was significantly reduced (about 4-fold reduction) compared with the Ad.Lz-infected control (Figs 1e and h). Furthermore, 3 days after infection, the levels of Nestin and MAP2 protein in Ad.SOCS3-infected cells significantly increased compared with the Ad.Lz-infected control, respectively (Figs 1e–g).

We then examined whether SOCS3 overexpression could affect the number of MAP2-positive neurons or GFAP-positive astrocytes (Figs 3a–d). Hoechst33342 staining was used to determine the number of individual nuclei in the total number of cells per visual field (400 μm^2). Cells that were positive for MAP2 or GFAP were scored in 10–15 random non-overlapping fields in each experiment. The proportion of MAP2- and GFAP-positive cells was expressed as a percentage of the MAP2- and GFAP-positive cells to Hoechst33342-positive cells, respectively. Each experiment was carried out five times. Figures 3e and f showed that SOCS3 overexpression significantly decreased the proportion of GFAP-positive cells (25.7 ± 3.0% of total cells [mean ± SD] in Ad.Lz vs. 9.3 ± 3.3% in Ad.SOCS3) and significantly increased the proportion of MAP2-positive cells (19.3 ± 1.2% of total cells [mean ± SD] in Ad.Lz vs. 29.1 ± 4.9% in Ad.SOCS3). These data suggest that overexpression of SOCS3 inhibited astrogliogenesis and promoted neurogenesis in neural stem cells.

© 2006 The Authors
Journal Compilation © 2006 International Society for Neurochemistry,

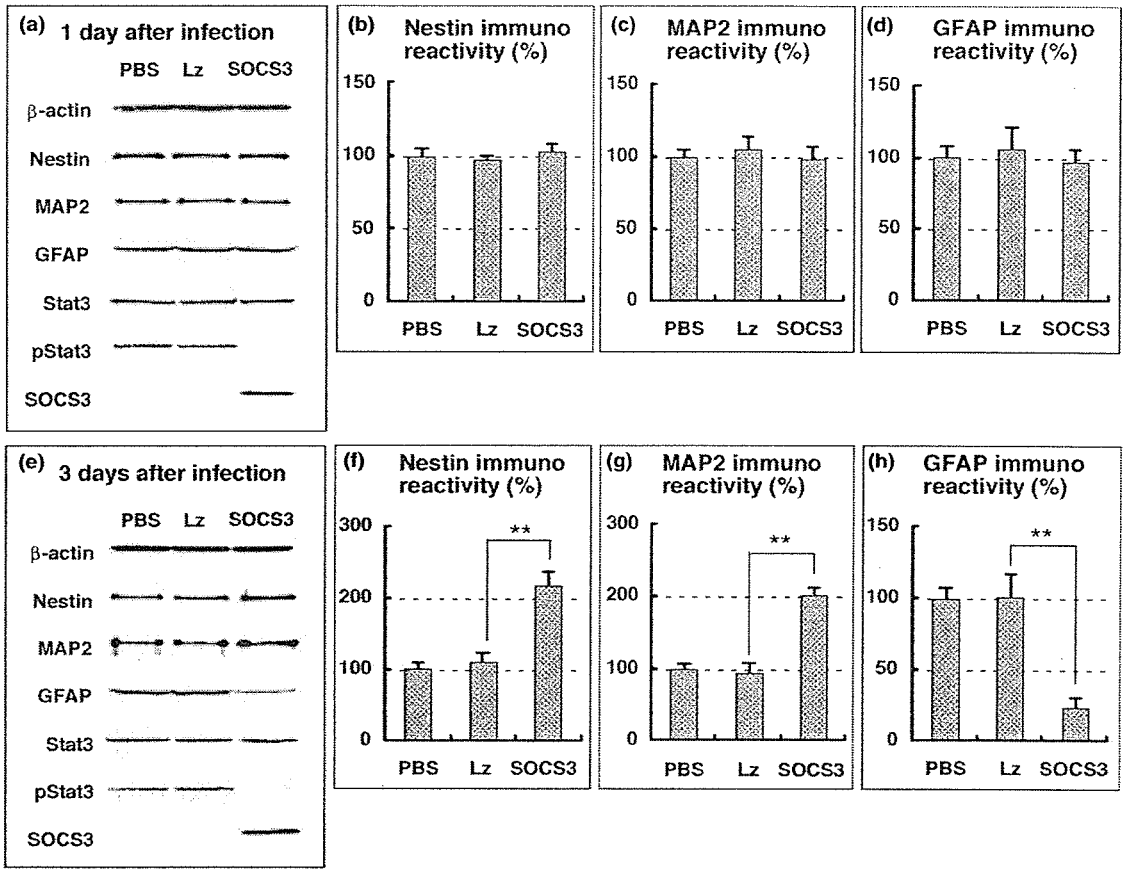

Fig. 1 Effects of SOCS3 on differentiation of neural stem cells 1 day or 3 days after infection. Neural stem cells were infected with adenoviral vectors expressing SOCS3 or β-galactosidase (Lz). One day or 3 days after viral infection, expression of each molecule was examined (a, e) and determined quantitatively (b–d: 1 day, f–h: 3 days). Data were obtained from five independent experiments. Values represent mean ± SD. Statistical significance was tested by one way ANOVA followed by Bonferroni's multiple comparison test. ** Significant difference vs. Lz-infected control ($p < 0.01$).

LIF-induced astrogliogenesis of the neural stem cells is inhibited by SOCS3

After confirming that LIF-induced Stat3 activation was completely inhibited by SOCS3, we examined the effects of SOCS3 on LIF + bFGF-induced differentiation of the neural stem cells. The neural stem cells were infected with adenoviral vector expressing SOCS3 or Lz (10 moi) for 1 h. One day later, the neural stem cells were treated with recombinant mouse LIF (30 ng/mL) and recombinant human bFGF (10 ng/mL). One day or 3 days after treatment, the cells were homogenized in lysis buffer and immunoblotted with an antibody against Nestin, GFAP, and MAP2. Densitometric analysis revealed that 1 day after treatment, Ad.Lz + LIF + bFGF-infected cells displayed an approximately 2.7-fold increase in GFAP protein level and an approximately 1.5-fold decrease in MAP2 protein level over the Ad.Lz-infected control (Figs 4a, c and d). In contrast, there was an approximately 5.0-fold decrease in GFAP protein level of the Ad.SOCS3 + LIF + bFGF-infected cells compared with the Ad.Lz + LIF + bFGF-infected cells and no difference in MAP2 protein level between these two groups (Figs 4a, c and d). These results suggest that SOCS3 primarily inhibited LIF-induced astrogliogenesis. Three days after treatment, Ad.Lz + LIF + bFGF-infected cells displayed an approximately 1.7-fold increase in GFAP protein level and an approximately 1.4-fold decrease in MAP2 protein level over the Ad.Lz-infected control level (Figs 4e, g and h). On the other hand, Ad.SOCS3 + LIF + bFGF-infected cells displayed an approximately 9.4-fold decrease in GFAP protein level and an approximately 1.7-fold increase in MAP2 protein level over the Ad.Lz-infected control (Figs 4e, g and h). In addition, 3 days after treatment, Ad.Lz + LIF + bFGF-infected cells displayed an approximately 1.5-fold increase, and Ad.SOCS3 + LIF + bFGF-infected cells displayed an approximately 2.4-fold increase in Nestin protein level over the Ad.Lz-infected control, respectively (Figs 4e, f).

Consistent with the previous report (Molne *et al.* 2000), our results showed that treatment of LIF + bFGF promoted astrogliogenesis and inhibited neurogenesis in the neural

© 2006 The Authors
Journal Compilation © 2006 International Society for Neurochemistry,

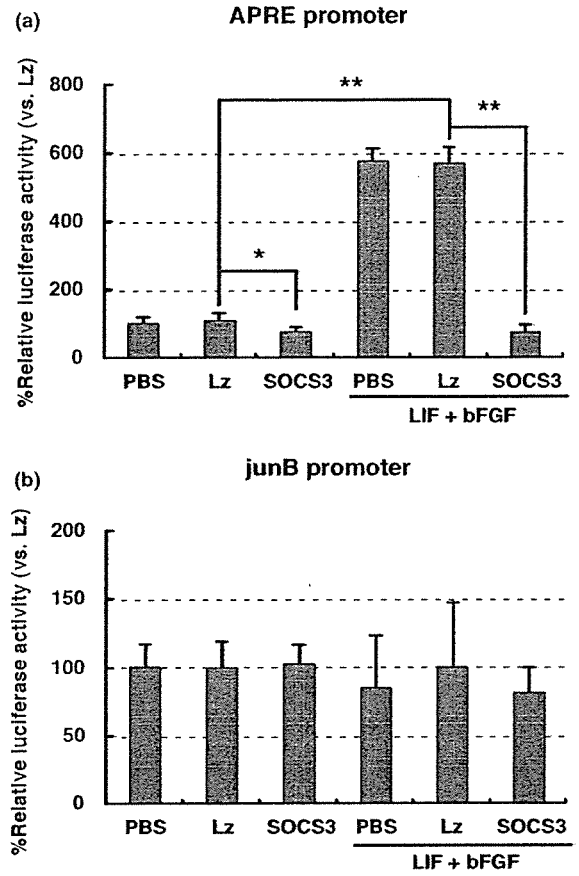

Fig. 2 Specific inhibition of Stat3 activity by Ad.SOCS3. Neural stem cells were transfected with (a) the Stat3 reporter plasmid (APRE) or (b) Stat3 control plasmid (junB). The transfected stem cells were infected with adenoviral vectors expressing SOCS3 (Ad.SOCS3) or β-galactosidase (Ad.Lz). One day later, the infected stem cells were treated with LIF (30 ng/mL) and bFGF (10 ng/mL) (LIF + bFGF) for 1 day. Then luciferase activities were evaluated using a Dual-luciferase assay kit (Promega). APRE promoter, Stat3 reporter plasmid containing four copies of acute phase responsive element in front of the minimal junB promoter linked to the luciferase gene. JunB promoter, Stat3 control plasmid containing the minimal junB promoter linked to the luciferase gene. Data were obtained from five independent experiments. Values were normalized to transfection efficiency and represent mean ± SD. Statistical significance was tested by one way ANOVA followed by Bonferroni's multiple comparison test. *, ** Significant difference ($p < 0.05$ and $p < 0.01$, respectively).

stem cells. As both SOCS3 and LIF + bFGF could up-regulate the level of Nestin protein, our results showed that SOCS3 mainly inhibited the role of LIF in neural stem cell differentiation.

SOCS3-positive stem cells express neither GFAP nor MAP2

Our observations that SOCS3 inhibited astrogliogenesis and promoted neurogenesis in the neural stem cells raised the question of whether SOCS3 expressing cells were differentiating into neurons or remained as stem cells. To address this inquiry, we performed the immunocytochemical experiment. Three days after infection, cells that were positive for Lz or SOCS3 were scored in 10–15 random non-overlapping fields in each experiment. The proportion of MAP2-positive cells was expressed as a percentage of the MAP2/Lz-double positive cells to Lz-positive cells or MAP2/SOCS3-double positive cells to SOCS3-positive cells, respectively. The proportion of GFAP-positive cells was expressed as a percentage of the GFAP/Lz- or GFAP/SOCS3-double positive cells to Lz- or SOCS3-positive cells, respectively. Each experiment was carried out four times. The proportion of the MAP2/Lz- or GFAP/Lz-double positive cells to Lz-positive cells (MAP2: 19.8 ± 5.6% of total Lz-positive cells; GFAP: 27.1 ± 3.3% of total Lz-positive cells) was almost the same as that of the MAP2- or GFAP-positive cells to Hoechst33342-positive cells (MAP2: 19.3 ± 1.2% of total cells [mean ± SD]; GFAP: 25.7 ± 3.0% of total cells), suggesting that overexpression of Lz had no influence on neural stem cell fate (Figs 5a–c, g). On the other hand, none of the SOCS3-positive cells expressed MAP2 or GFAP proteins, although all of the SOCS3-positive cells expressed Nestin protein (Figs 5d–f, h). These results suggested that SOCS3 expressing cells remained as neural stem cells.

RT-PCR for Notch family members and inhibitory bHLH factors

Notch family members and inhibitory bHLH transcription factors play important roles in proliferation, cell lineage determination and cell differentiation of neural stem cells (Lasky and Wu 2005). We therefore examined the effects of SOCS3 overexpression on the mRNA expression of Notch family members (notch1, 2 and 3) as well as inhibitory bHLH transcription factors (hes1, hes5, id1, id2 and id3) in neural stem cells. Analysis by RT-PCR revealed that the mRNA levels of notch1, hes5 and id3 in Ad.SOCS3-infected cells increased significantly (1.4-fold, 1.5-fold and 1.4-fold increase, respectively), compared with the Ad.Lz-infected control level 1 day after infection (Figs 6a and b). Three days after infection, the mRNA levels of notch1 and id3 were still up-regulated by SOCS3 overexpression (Figs 7a and b). However, the mRNA level of hes5 was reduced significantly (4-fold reduction) compared with the Ad.Lz-infected control level (Figs 7a and b). As notch has been reported to maintain 'definitive' neural stem cells (Hitoshi *et al.* 2004), our results suggested that SOCS3 could maintain neural stem cells through the up-regulation of notch1.

RT-PCR for bHLH determination factors, bHLH differentiation factors and Sox9

To confirm that SOCS3 can induce neurogenesis in neural stem cells, we examined the effects of SOCS3 on the expression of the bHLH determination factor (mash1), bHLH

© 2006 The Authors
Journal Compilation © 2006 International Society for Neurochemistry,

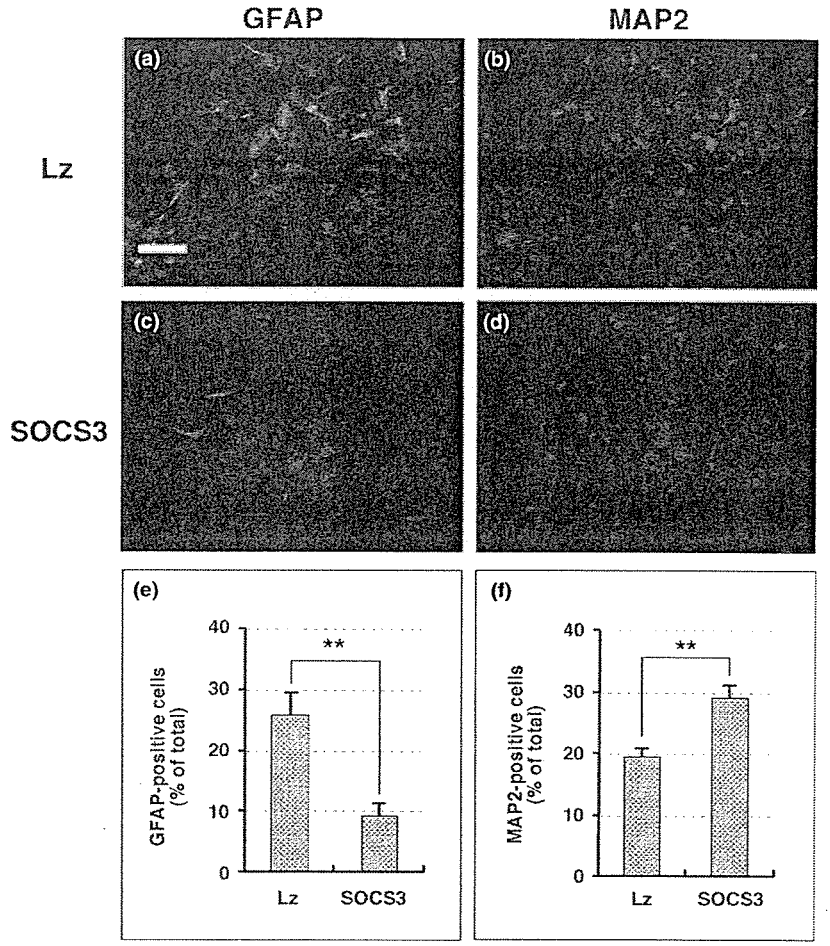

Fig. 3 Effects of SOCS3 on differentiation of neural stem cells 3 days after infection. Neural stem cells were infected with an adenoviral vector expressing SOCS3 or β-galactosidase (Lz). Three days later, expression of differentiation markers was evaluated by immunostaining with antibody against GFAP (a, c: green) or MAP2 (b, d: red). Hec, Hoechst33342 nuclear staining (blue). Bar = 100 μm. Data were obtained from five independent measurements. Values represent mean ± SD. ** Significant difference vs. Lz-infected control ($p < 0.01$).

differentiation factors (neuroD1 and neuroD2), and sox9. Analysis by RT-PCR revealed no changes in the mRNA levels of mash1 and sox9 1 day or 3 days after infection (Figs 6c–d and 7c–d). The mRNA levels of neuroD1 and neuroD2 in Ad.SOCS3-infected cells increased significantly (1.6-fold and 1.8-fold increase, respectively) compared with the Ad.Lz-infected control level 1 day after infection (Figs 6c, d). Three days after infection, the mRNA levels of neuroD1 and neuroD2 remained up-regulated. These data suggest that overexpression of SOCS3 promoted terminal neural differentiation of neural stem cells.

AG490 inhibits astrogliogenesis in the neural stem cells and promotes expressions of Notch1 and Notch3 mRNA

To confirm that up-regulations of notch1 were involved in Jak/Stat cell signaling machinery, we applied AG490, a JAK2 kinase inhibitor, and evaluated the neural stem cell fate and the alteration of Notch mRNA expression. Treatment with AG490 significantly decreased the GFAP protein level of the Ad.Lz-infected stem cells (Figs 8a and c). However, no significant difference in the MAP2 protein level of the Ad.Lz-infected stem cells could be detected after AG490 treatment (Figs 8a and b). One day after treatment, there was an approximately 2.2-fold increase in the notch1 mRNA level and a 5.4-fold increase in the notch3 mRNA level of Ad.Lz-infected stem cells (Fig. 8d). Three days after treatment, the mRNA levels of notch1 and notch3 remained up-regulated (Fig. 8e). These results showed that inhibition of Jak/Stat cell signaling machinery could inhibit the astrogliogenesis and up-regulate both notch1 and notch3 mRNA expression.

Discussion

In the present study, we demonstrated that overexpression of SOCS3 promoted neurogenesis and inhibited astrogliogenesis in neural stem cells. Promoter assay with Stat3 reporter plasmids revealed that transcriptional activity of Stat3 was significantly suppressed after overexpression of SOCS3 in neural stem cells, whereas transcriptional activity of Stat3 was markedly increased in the presence of LIF and bFGF. These results are in good agreement with the general notion that activation of Stat3 in neural stem cells results in

© 2006 The Authors

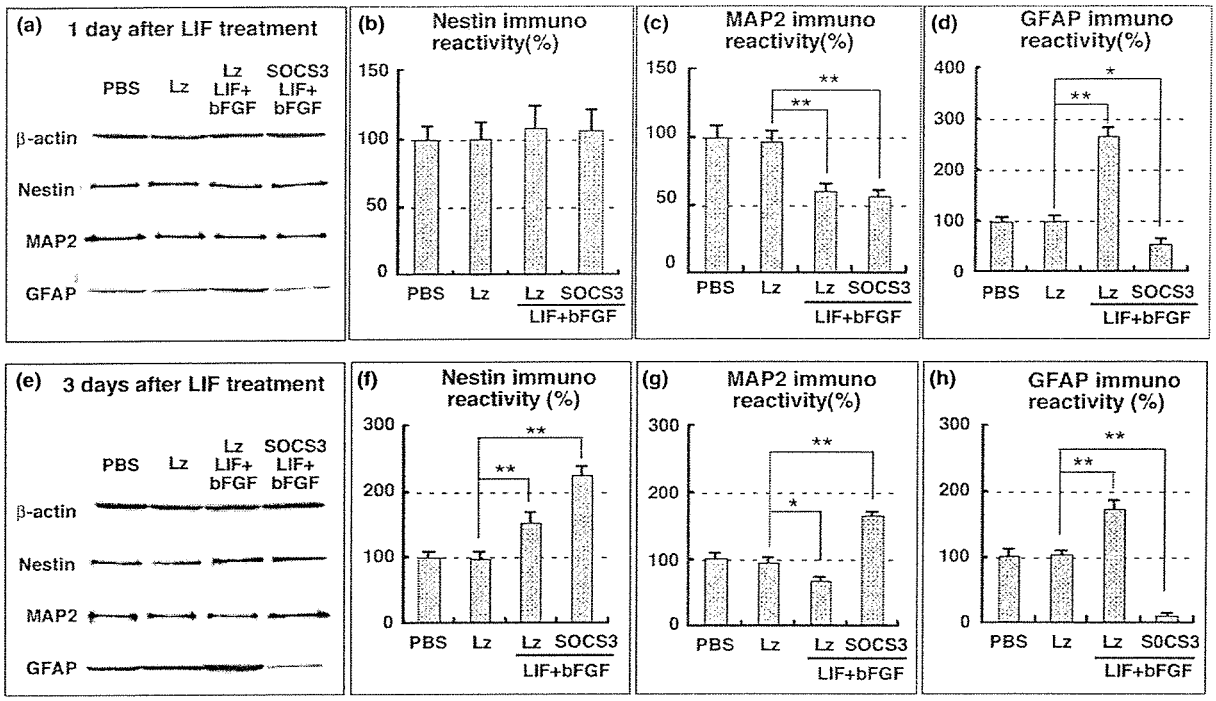

Fig. 4 Effects of SOCS3 on LIF + bFGF-induced differentiation of neural stem cells 1 day and 3 days after treatment. Neural stem cells were infected with adenoviral vectors expressing SOCS3 or β-galactosidase (Lz). One day later, the infected stem cells were treated with LIF (30 ng/mL) and bFGF (10 ng/mL) (LIF + bFGF). One day or 3 days after the treatment, expression of each molecule was examined (a, e) and determined quantitatively (b–d: 1 day, f–h: 3 days). Data were obtained from five independent experiments. Values represent mean ± SD. Statistical significance was tested by one way ANOVA followed by Bonferroni's multiple comparison test. *, ** Significant difference vs. Lz-infected control ($p < 0.05$ and $p < 0.01$, respectively).

subsequent glial differentiation. In fact, we reported previously that overexpression of the dominant negative form of Stat3 (Stat3F) results in promotion of neurogenesis and inhibition of astrogliogenesis in neural stem cells (Gu *et al.* 2005). In that report, mRNA levels of Notch family members (Notch1, 2 and 3) and inhibitory bHLH transcriptional factors (Hes5, Id2 and Id3) were significantly decreased after overexpression of Stat3F, suggesting differentiation of neural stem cells. In the present study, however, RT-PCR analysis revealed that mRNA levels of Notch1, Hes5 and Id3 increased significantly 1 day after overexpression of SOCS3, suggesting maintenance of a neural stem cell state. In accordance with this result, the protein level of Nestin (a specific marker of neural stem cells) was also significantly increased after overexpression of SOCS3.

Notch is thought to control cellular differentiation by lateral inhibition, which ensures that two distinct cell types are produced in correct numbers from a population of initially equipotent cells (Beatus and Lendahl 1998). Although the equipotent cells initially express equivalent levels of both ligands and receptors, the Notch-responding cell down-regulates its own ligand expression effectively by a negative feedback mechanism and vice versa. This 'standard lateral inhibition' is therefore a general strategy for preventing all equipotent cells from having the same fate, and cells in which Notch is activated will remain as progenitors to participate in subsequent waves of differentiation (Hitoshi *et al.* 2004). Inductive signaling, on the other hand, involves the Notch receptor and ligand expressed on two different cell types, such that Notch is only activated in receptor-bearing cells. Notch signaling then creates a new cell type as a result of cell–cell interactions at the boundary between distinct cell populations. This role of Notch signaling has been demonstrated in mammalian gliogenesis (Gaiano and Fishell 2002). Increasing evidence suggests that Notch-mediated signaling pathways are crucial for mammalian CNS development via maintenance of a neural stem cell (progenitor) state, inhibition of neuronal commitment, and promotion of glial fate (Lasky and Wu 2005). As notch has been reported to maintain 'definitive' neural stem cells (Hitoshi *et al.* 2004), our RT-PCR results suggested that SOCS3 could maintain neural stem cells through the up-regulation of notch1.

Furthermore, we showed that all SOCS3-positive cells expressed Nestin protein but neither MAP2 nor GFAP protein. Our western blot results revealed that SOCS3 up-

© 2006 The Authors
Journal Compilation © 2006 International Society for Neurochemistry,

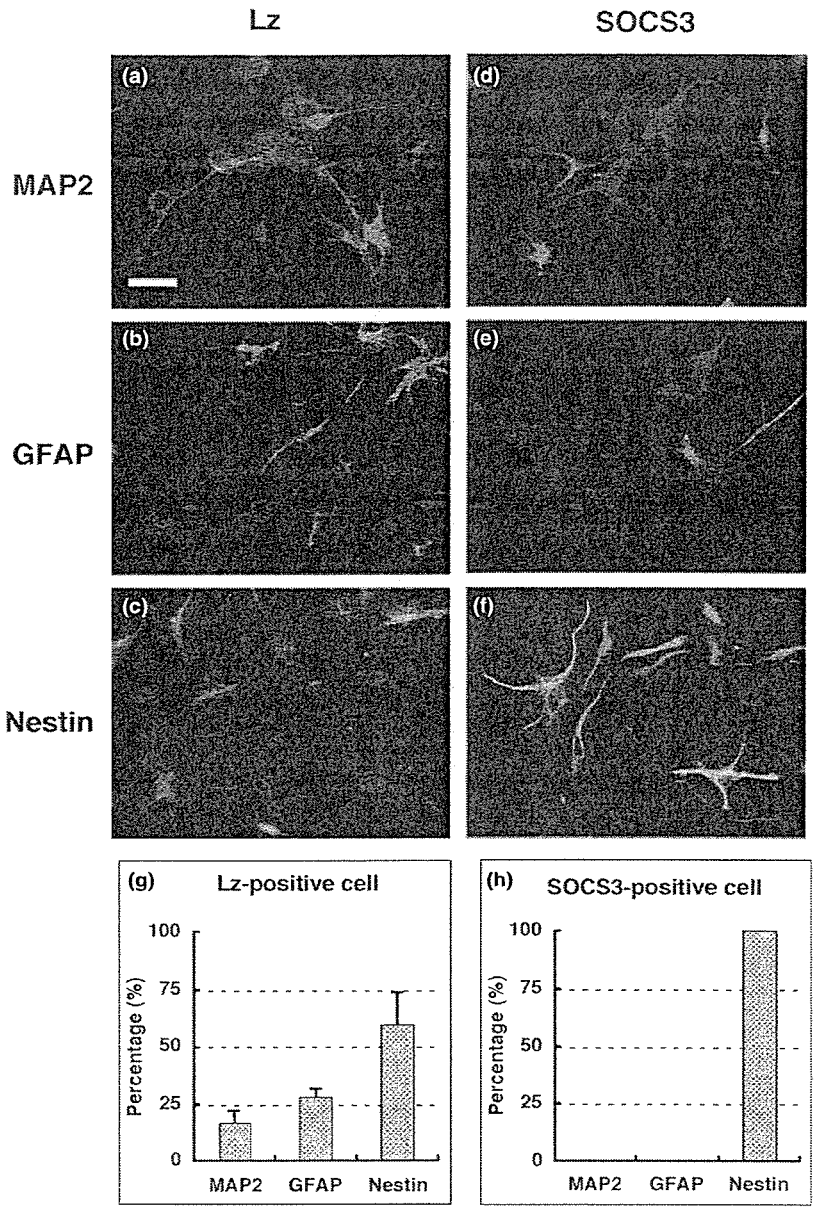

Fig. 5 Effects of SOCS3 on differentiation of neural stem cells 3 days after infection. Neural stem cells were infected with an adenoviral vector expressing SOCS3 or β-galactosidase (Lz). Three days later, expression of Lz (a–c; red), SOCS3 (d–f; red) and cell markers – MAP2 (a, d: green), GFAP (b, e: green), and Nestin (c, f: green) was evaluated immunocytochemically. Note that SOCS3-positive cells expressed neither MAP2 (d) nor GFAP (e). Bar = 40 μm. Data were obtained from five independent measurements. Values represent mean ± SD.

regulated the expression of Nestin protein in the neural stem cells. These results also suggested that SOCS3 promoted maintenance in the neural stem cells. However, our other experiments showed that overexpression of SOCS3 promoted neurogenesis in neural stem cells. The reason for this discrepancy is not clear. One possibility is that SOCS3 can eventually lead to neurogenesis without affecting the Jak/Stat signaling (Rakesh and Agrawal 2005). In fact, it has been reported that SOCS2, another family of SOCS proteins, directly regulates the differentiation of neural stem cells into neurons (Turnley *et al.* 2002). Progenitors lacking SOCS2 produced more astrocytes *in vitro*, and mice lacking SOCS2 have fewer neurons *in vivo*, whereas SOCS2 overexpression increases neural differentiation of neural stem cells (Turnley *et al.* 2002). Similarly, there was an increase in neuron-like cell differentiation when primary cortical cells were transfected with SOCS3 (Yadav *et al.* 2005). The second possibility is that SOCS3-positive cells secrete some unknown factors to promote neurogenesis through paracrine system. The third possibility is that SOCS3 indirectly regulates the differentiation of neural stem cells into neurons. Our data showed that SOCS3 promoted maintenance of neural stem cell and inhibited astrogliogenesis. In the present study, we have used the differentiating

© 2006 The Authors
Journal Compilation © 2006 International Society for Neurochemistry,

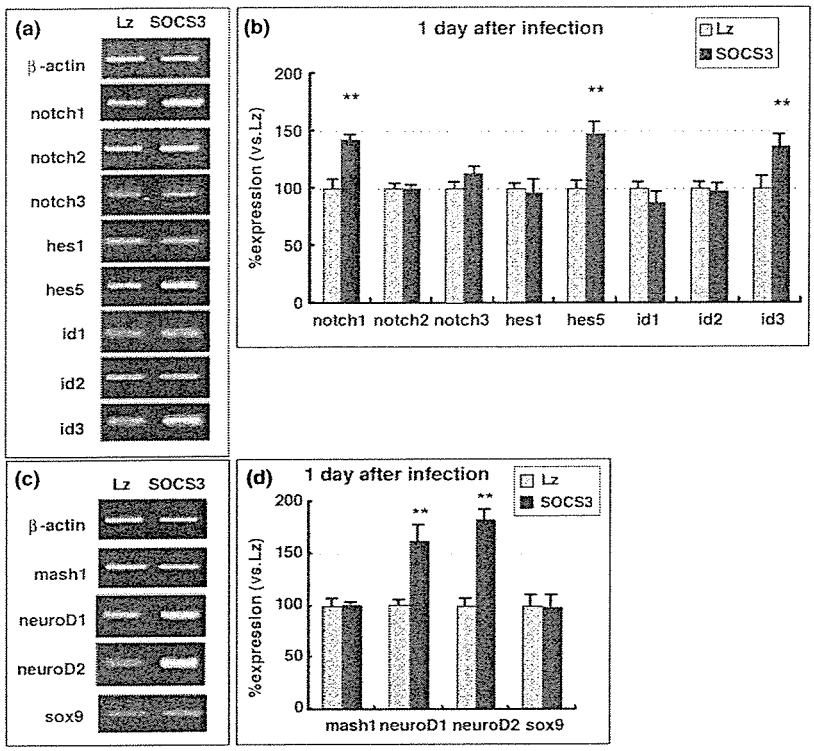

Fig. 6 Effects of SOCS3 on mRNA expression of Notch family members, bHLH transcription factors and Sox9 1 day after infection. RNA was extracted from cells 1 day after infection with adenoviral vectors expressing SOCS3 or β-galactosidase (Lz). RT-PCR analyses were conducted to examine mRNA levels of Notch family members (Notch1, 2 and 3), inhibitory bHLH transcription factors (Hes1, Hes5, Id1, Id2 and Id3), proneuronal bHLH transcription factors (Mash1, NeuroD1 and NeuroD2) and Sox9. Data were obtained from five independent measurements. Values represent mean ± SD. ** Significantly greater than Lz-infected control ($p < 0.01$).

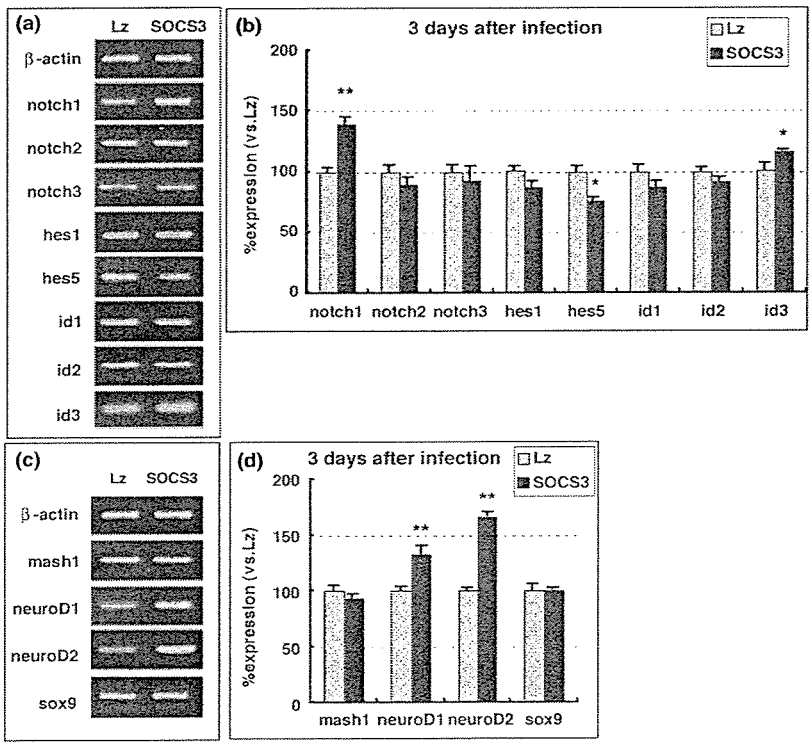

Fig. 7 Effects of SOCS3 on mRNA expression of Notch family members, bHLH transcription factors and Sox9 3 days after infection. RNA was extracted from cells 3 days after infection with adenoviral vectors expressing SOCS3 or β-galactosidase (Lz). RT-PCR analyses were conducted to examine mRNA levels of Notch family members (Notch1, 2 and 3), inhibitory bHLH transcription factors (Hes1, Hes5, Id1, Id2 and Id3), proneuronal bHLH transcription factors (Mash1, NeuroD1 and NeuroD2) and Sox9. Values represent mean ± SD. *, ** Significant difference vs. Lz-infected control ($p < 0.05$ and $p < 0.01$, respectively).

medium containing retinoic acid, which has been reported to be a differentiation factor involved in the development of the CNS (Goncalves *et al.* 2005). For the maintenance of neural stem cells mediated by Notch, some of the progenitor cells are forced to be differentiated through the mechanism of 'standard lateral inhibition'. Consequently, progenitor

© 2006 The Authors
Journal Compilation © 2006 International Society for Neurochemistry,

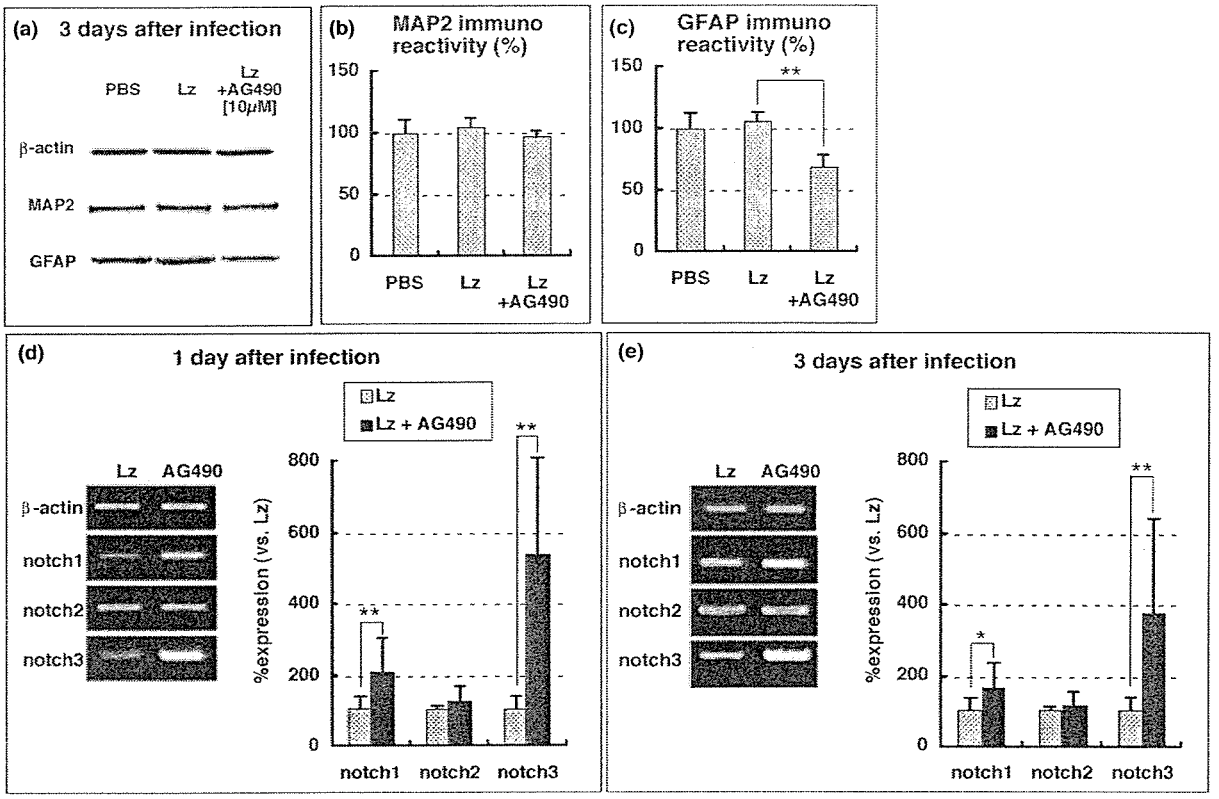

Fig. 8 Effects of AG490 on neural stem cell fate and mRNA expression of Notch family members. Neural stem cells were infected with adenoviral vectors expressing β-galactosidase (Lz) in the presence and absence of AG490 (10 μM). Three days after viral infection, expression of each molecule was examined (a) and determined quantitatively (b and c). One day and 3 days after infection, RNA was extracted from the infected stem cells and RT-PCR analyses were conducted to examine mRNA levels of Notch family members (Notch1, 2 and 3) (d: 1 day; e: 3 days). Data were obtained from four independent experiments. Values represent mean ± SD. *, ** Significant difference vs. Lz-infected control ($p < 0.05$ and $p < 0.01$, respectively).

cells that are forced to be differentiated may be inevitably differentiated to neurons, appearing to promote neurogenesis. The last explanation may be preferable, because we showed that at early stage, SOCS3 inhibited the LIF-induced astrogliogenesis in the neural stem cells but did not promote neurogenesis, and that the suppression of Jak-Stat pathway by AG490 inhibited astrogliogenesis in neural stem cells without promoting neurogenesis. Further cellular and molecular biological investigations are required to clarify the mechanism of SOCS3-induced neurogenesis.

In addition, our data showed that overexpression of SOCS3 promoted not only neurogenesis but also maintenance of neural stem cells. This method can be applied to stem cell replacement therapy. Stem cell replacement therapy has been proposed as a means of replacing specific populations of cells lost through trauma, disease or ageing. Neural stem cells are capable of unlimited self-renewal, and can differentiate into cells of the CNS, providing a relatively unlimited source of cells for transplantation if appropriate differentiation protocols to generate highly enriched populations of neural cells can be developed. However, the appropriate culture conditions that allow the long-term expansion of therapeutically important neural populations have not been developed (Taylor and Minger 2005). When expanded several times, the proportion of neurons declines significantly at the expense of increasing glial cell number. Overexpression of SOCS3 in neural stem cells might overcome these problems.

Finally, the immunogenic and cytopathic effects of adenoviral vectors limit their use (St George 2003). In fact, exposing neurospheres to recombinant adenoviral vectors has resulted in differentiation into astrocytes, even in the presence of EGF (Hughes *et al.* 2002). However, astrogliogenesis of neurospheres was not apparent after exposure to a viral vector that expressed β-galactosidase, at the dosage used in this study. Instead, neurogenesis was apparent in the Ad.SOCS3-infected group, compared with the Ad.Lz-infected group exposed to the same vector titer. Thus, our findings were not due to compromising effects of the adenoviral vector.

© 2006 The Authors
Journal Compilation © 2006 International Society for Neurochemistry,

Acknowledgements

We are grateful to Ms K. Hiraoka for her secretarial assistance. The present study was supported in part by a grant-in-aid from the Ministry of Education, Science and Culture and by a grant-in-aid from Daiwa Securities Health Foundation and Mitsui Sumitomo Insurance Welfare Foundation.

References

Beatus P. and Lendahl U. (1998) Notch and neurogenesis. *J. Neurosci. Res.* **54**, 125–136.

Bonni A., Sun Y., Nadal-Vicens M., Bhatt A., Frank D. A., Rozovsky I., Stahl N., Yancopoulos G. D. and Greenberg M. E. (1997) Regulation of gliogenesis in the central nervous system by the JAK-STAT signaling pathway. *Science* **278**, 477–483.

Gaiano N. and Fishell G. (2002) The role of notch in promoting glial and neural stem cell fates. *Annu. Rev. Neurosci.* **25**, 471–490.

Gangemi R. M., Perera M. and Corte G. (2004) Regulatory genes controlling cell fate choice in embryonic and adult neural stem cells. *J. Neurochem.* **89**, 286–306.

Goncalves M. B., Boyle J., Webber D. J., Hall S., Minger S. L. and Corcoran J. P. (2005) Timing of the retinoid-signalling pathway determines the expression of neuronal markers in neural progenitor cells. *Dev Biol.* **278**, 60–70.

Gu F., Hata R., Toku K., Yang L., Ma Y. J., Maeda N., Sakanaka M. and Tanaka J. (2003) Testosterone up-regulates aquaporin-4 expression in cultured astrocytes. *J. Neurosci. Res.* **72**, 709–715.

Gu F., Hata R., Ma Y. J., Tanaka J., Mitsuda N., Kumon Y., Hanakawa Y., Hashimoto K., Nakajima K. and Sakanaka M. (2005) Suppression of Stat3 promotes neurogenesis in cultured neural stem cells. *J. Neurosci. Res.* **81**, 163–171.

Hitoshi S., Seaberg R. M., Koscik C., Alexson T., Kusunoki S., Kanazawa I., Tsuji S. and van der Kooy D. (2004) Primitive neural stem cells from the mammalian epiblast differentiate to definitive neural stem cells under the control of Notch signaling. *Genes Dev.* **18**, 1806–1811.

Hughes S. M., Moussavi-Harami F., Sauter S. L. and Davidson B. L. (2002) Viral-mediated gene transfer to mouse primary neural progenitor cells. *Mol. Ther.* **5**, 16–24.

Johe K. K., Hazel T. G., Muller T., Dugich-Djordjevic M. M. and McKay R. D. (1996) Single factors direct the differentiation of stem cells from the fetal and adult central nervous system. *Genes Dev* **10**, 3129–3140.

Kanegae Y., Makimura M. and Saito I. (1994) A simple and efficient method for purification of infectious recombinant adenovirus. *Jpn J. Med. Sci. Biol.* **47**, 157–166.

Lang R., Pauleau A. L., Parganas E., Takahashi Y., Mages J., Ihle J. N., Rutschman R. and Murray P. J. (2003) SOCS3 regulates the plasticity of gp130 signaling. *Nat. Immunol.* **4**, 546–550.

Lasky J. L. and Wu H. (2005) Notch signaling, brain development, and human disease. *Pediatr Res.* **57**, 104R–109R.

Levy D. E. and Lee C. K. (2002) What does Stat3 do? *J. Clin. Invest.* **109**, 1143–1148.

Molne M., Studer L., Tabar V., Ting Y. T., Eiden M. V. and McKay R. D. (2000) Early cortical precursors do not undergo LIF-mediated astrocytic differentiation. *J. Neurosci. Res.* **59**, 301–311.

Nakajima K., Yamanaka Y., Nakae K., Kojima H., Ichiba M., Kiuchi N., Kitaoka T., Fukada T., Hibi M. and Hirano T. (1996) A central role for Stat3 in IL-6-induced regulation of growth and differentiation in M1 leukemia cells. *EMBO J.* **15**, 3651–3658.

Nakashima K., Yanagisawa M., Arakawa H., Kimura N., Hisatsune T., Kawabata M., Miyazono K. and Taga T. (1999) Synergistic signaling in fetal brain by STAT3-Smad1 complex bridged by p300. *Science* **284**, 479–482.

Nicholson S. E., De Souza D., Fabri L. J. *et al.* (2000) Suppressor of cytokine signaling-3 preferentially binds to the SHP-2-binding site on the shared cytokine receptor subunit gp130. *Proc. Natl Acad. Sci. U S A* **97**, 6493–6498.

Rajan P. and McKay R. D. (1998) Multiple routes to astrocytic differentiation in the CNS. *J. Neurosci.* **18**, 3620–3629.

Rakesh K. and Agrawal D. K. (2005) Controlling cytokine signaling by constitutive inhibitors. *Biochem. Pharmacol.* **70**, 649–657.

Ross S. E., Greenberg M. E. and Stiles C. D. (2003) Basic helix-loop-helix factors in cortical development. *Neuron* **39**, 13–25.

Schmitz J., Weissenbach M., Haan S., Heinrich P. C. and Schaper F. (2000) SOCS3 exerts its inhibitory function on interleukin-6 signal transduction through the SHP2 recruitment site of gp130. *J. Biol. Chem.* **275**, 12 848–12 856.

Shouda T., Yoshida T., Hanada T *et al.*. (2001) Induction of the cytokine signal regulator SOCS3/CIS3 as a therapeutic strategy for treating inflammatory arthritis. *J. Clin. Invest.* **108**, 1781–1788.

St George J. A. (2003) Gene therapy progress and prospects: adenoviral vectors. *Gene Ther* **10**, 1135–1141.

Starr R., Willson T. A., Viney E. M., Murray L. J., Rayner J. R., Jenkins B. J., Gonda T. J., Alexander W. S., Metcalf D., Nicola N. A. and Hilton D. J. (1997) A family of cytokine-inducible inhibitors of signalling. *Nature* **387**, 917–921.

Stolt C. C., Lommes P., Sock E., Chaboissier M. C., Schedl A. and Wegner M. (2003) The Sox9 transcription factor determines glial fate choice in the developing spinal cord. *Genes Dev.* **17**, 1677–1689.

Sun Y. E., Martinowich K. and Ge W. (2003) Making and repairing the mammalian brain – signaling toward neurogenesis and gliogenesis. *Semin. Cell Dev. Biol.* **14**, 161–168.

Takizawa T., Nakashima K., Namihira M., Ochiai W., Uemura A., Yanagisawa M., Fujita N., Nakao M. and Taga T. (2001) DNA methylation is a critical cell-intrinsic determinant of astrocyte differentiation in the fetal brain. *Dev. Cell* **1**, 749–758.

Taylor H. and Minger S. L. (2005) Regenerative medicine in Parkinson's disease: generation of mesencephalic dopamingeric cells from embryonic stem cells. *Curr. Opin. Biotechnol.* **16**, 487–492.

Turnley A. M., Faux C. H., Rietze R. L., Coonan J. R. and Bartlett P. F. (2002) Suppressor of cytokine signaling 2 regulates neuronal differentiation by inhibiting growth hormone signaling. *Nat. Neurosci.* **5**, 1155–1162.

Yadav A., Kalita A., Dhillon S. and Banerjee K. (2005) JAK/STAT3 pathway is involved in survival of neurons in response to insulin-like growth factor and negatively regulated by suppressor of cytokine signaling-3. *J. Biol. Chem.* **280**, 31 830–31 840.

Yoshimura A., Nishinakamura H., Matsumura Y. and Hanada T. (2005) Negative regulation of cytokine signaling and immune responses by SOCS proteins. *Arthritis Res. Ther.* **7**, 100–110.

© 2006 The Authors
Journal Compilation © 2006 International Society for Neurochemistry,

ORIGINAL ARTICLE

See related commentary on pg 510

Antimicrobial Peptides Human β-Defensins Stimulate Epidermal Keratinocyte Migration, Proliferation and Production of Proinflammatory Cytokines and Chemokines

François Niyonsaba[1], Hiroko Ushio[1], Nobuhiro Nakano[1], William Ng[1,2], Koji Sayama[3], Koji Hashimoto[3], Isao Nagaoka[4], Ko Okumura[5] and Hideoki Ogawa[1]

Besides their microbicidal functions, human β-defensins (hBD) and LL-37 activate different immune and inflammatory cells, and their expression is enhanced in inflamed skin and cutaneous wound sites. To protect against pathogens, the skin produces antimicrobial peptides including hBDs and LL-37. Therefore, the aim of our study was to investigate whether hBDs participate in cutaneous inflammation and wound healing by inducing keratinocyte migration, proliferation, and production of proinflammatory cytokines/chemokines. We found that hBD-2, -3, and -4 but not hBD-1 stimulated human keratinocytes to increase their gene expression and protein production of IL-6, IL-10, IP-10, monocyte chemoattractant protein-1, macrophage inflammatory protein-3α, and RANTES. This stimulatory effect was markedly suppressed by pertussis toxin and U-73122, inhibitors for G protein and phospholipase C, respectively. We also demonstrated that hBDs elicited intracellular Ca^{2+} mobilization, and increased keratinocyte migration, and proliferation. In addition, these peptides induced phosphorylation of EGFR, signal transducer and activator of transcription (STAT)1, and STAT3, which are intracellular signaling molecules involved in keratinocyte migration and proliferation. In our study, inhibition of these molecules significantly reduced hBD-mediated keratinocyte migration and proliferation. In conclusion, this study provides evidence that human antimicrobial peptides may be involved in skin immunity through stimulating cytokine/chemokine production, and participate in wound healing by promoting keratinocyte migration and proliferation.

Journal of Investigative Dermatology (2007) **127**, 594–604. doi:10.1038/sj.jid.5700599; published online 19 October 2006

INTRODUCTION

The skin generates a number of antimicrobial peptides that form part of innate immunity of the epithelial barrier. The major antimicrobial peptides found in humans are defensins and cathelicidins, which inactivate and kill invading microorganisms (Lehrer and Ganz, 1999). Defensins are characterized by six cysteine residues forming three intramolecular disulfide bridges, and are divided into the α- and β-defensins based on the distribution of the cysteines and linkages of the disulfide bonds. Six human α-defensins have been identified; four of them named human neutrophil peptides 1–4 are generated by neutrophils, and the other two termed human defensins-5 and -6 are produced and stored in the secretory granules of intestinal Paneth cells (Oppenheim *et al.*, 2003).

In contrast to α-defensins, human β-defensins (hBD) are mainly generated by epithelial tissues including skin and respiratory tract. So far, four hBDs namely, hBD-1, -2, -3, and -4 have been identified in human skin (Fulton *et al.*, 1997; Harder *et al.*, 1997, 2001, 2004; Ali *et al.*, 2001; Oppenheim *et al.*, 2003). hBD-1 is constitutively produced by various epithelial tissues, its expression is especially prominent in terminal layers of the skin (Fulton *et al.*, 1997; Ali *et al.*, 2001), and may be induced by lipopolysaccharide and peptidoglycan in keratinocytes (Sørensen *et al.*, 2005). hBD-2 was originally isolated from extracts of lesional scales from psoriatic skin, and is inducible in inflamed skin lesions upon treatment with lipopolysaccharide, tumor necrosis factor-α, IL-1β, and bacteria (Harder *et al.*, 1997; Liu *et al.*,

[1]*Atopy (Allergy) Research Center, Juntendo University School of Medicine, Tokyo, Japan;* [2]*Department of Dermatology, Juntendo University School of Medicine, Tokyo, Japan;* [3]*Department of Dermatology, Ehime University School of Medicine, Ehime, Japan;* [4]*Department of Host Defense and Biochemical Research, Juntendo University School of Medicine, Tokyo, Japan and* [5]*Department of Immunology, Juntendo University School of Medicine, Tokyo, Japan*

Correspondence: Dr François Niyonsaba, Atopy (Allergy) Research Center, Juntendo University School of Medicine, 2-1-1 Hongo, Bunkyo-ku, Tokyo 113-8421, Japan. E-mail: francois@med.juntendo.ac.jp

Abbreviations: CCK, cell-counting kit-8; hBD, human β-defensin; PTx, pertussis toxin; mRNA, messenger RNA; PBS, phosphate-buffered saline; PLC, phospholipase C; SD, standard deviation; siRNA, small-interfering RNA; STAT, signal transducer and activator of transcription; TGF, transforming growth factor

Received 18 April 2006; revised 25 July 2006; accepted 31 August 2006; published online 19 October 2006

© 2006 The Society for Investigative Dermatology

2002). hBD-2 is localized to the uppermost layers of the epidermis (Huh *et al.*, 2002; Oren *et al.*, 2003), and the levels of hBD-2 dramatically increase in differentiated keratinocytes (Harder *et al.*, 2004). Furthermore, it has been demonstrated that hBD-2 is synthesized and stored in lamellar bodies of keratinocytes of the spinous and granular layers (Huh *et al.*, 2002; Oren *et al.*, 2003). hBD-3 was detected by screening human genomic sequences (García *et al.*, 2001a; Jia *et al.*, 2001), and successively isolated from human lesional psoriatic scales (Harder *et al.*, 2001). This peptide has been found in both epithelial and non-epithelial tissues (García *et al.*, 2001a). The expression of hBD-3 is upregulated in keratinocytes and epithelia of the respiratory, gastrointestinal, and genito-urinary tracts upon stimulation by tumor necrosis factor-α, IL-1β, IFN-γ, and bacteria (Harder *et al.*, 2001; García *et al.*, 2001a). The fourth member of hBDs, hBD-4, was initially identified by screening the human genome database (García *et al.*, 2001b). It is upregulated by infection with bacteria and phorbol 12-myristate 13-acetate in epithelial cells (García *et al.*, 2001b). The gene expression of hBD-4 is inducible in primary keratinocytes (Harder *et al.*, 2004).

In addition to hBDs, the skin epithelium also generates cathelicidins, which are a family of antimicrobial peptides containing a highly conserved N-terminal cathelin domain and a C-terminal cationic antimicrobial domain that becomes active after cleavage (Zanetti *et al.*, 1995). Although many cathelicidin members have been identified in mammalians, only one cathelicidin LL-37 is present in humans. LL-37 was identified in myeloid cells, and later shown to be expressed in various epithelia and particularly in keratinocytes of inflamed skin (Sørensen *et al.*, 1997, Frohm *et al.*, 1999).

Apart from their direct microbicidal functions, antimicrobial peptides are known to activate several types of human cells. hBD stimulate the degranulation of mast cells (Befus *et al.*, 1999) and chemoattract monocytes, and T cells (Chertov *et al.*, 1996). Furthermore, hBDs and LL-37 are chemotaxins for immune and inflammatory cells (Yang *et al.*, 1999, 2000; Niyonsaba *et al.*, 2002a, b, 2004). In addition, these peptides are involved in the production of proinflammatory mediators such as histamine and prostaglandin D_2 from mast cells (Niyonsaba *et al.*, 2001), and IL-18 by keratinocytes (Niyonsaba *et al.*, 2005).

The ability of the skin to protect against pathogens has been in part attributed to the presence of antimicrobial agents such as hBDs and LL-37 that have been shown to play major roles in the innate immune system. Moreover, the expression of LL-37 has been demonstrated to be enhanced in wounds (Dorschner *et al.*, 2001), and α-defensins as well as LL-37 have been reported to be involved in cell proliferation and wound closure in airway epithelium (Aarbiou *et al.*, 2002, 2004; Shaykhiev *et al.*, 2005). The wound closure process is initiated by a series of cellular activities such as cell migration, proliferation, and differentiation (Zahm *et al.*, 2000). It was the aim of the current study to characterize the roles of hBDs in activation of keratinocytes and induction of cell migration and proliferation. We found that hBD-2, -3, and -4 but not hBD-1 stimulated gene expression and production of various proinflammatory cytokines and chemokines by human primary keratinocytes. Moreover, the production of these cytokines/chemokines was mediated through the G protein and phospholipase C (PLC) signaling pathway. In addition, we revealed that hBDs increased the migration and proliferation of keratinocytes mediated by EGFR, signal transducer and activator of transcription (STAT)1 and STAT3, molecules involved in keratinocyte migration and proliferation (Sano *et al.*, 1999). Furthermore, hBDs were also able to induce phosphorylation of EGFR, STAT1, and STAT3.

RESULTS

hBDs increase the gene expression of proinflammatory cytokines and chemokines

To investigate the effects of human antimicrobial peptides in the skin, we first analyzed whether hBDs could induce the messenger RNA (mRNA) expression of various proinflammatory cytokines and chemokines from keratinocytes. Human primary keratinocytes were incubated with 30 μg/ml of hBD-1, -2, -3, and -4 for 1–24 hours, and gene expression was analyzed using real-time PCR. Among the cytokines and chemokines investigated, we revealed that hBD-2, -3, and -4 significantly induced the mRNA expression of IL-6, IL-10, IFN-γ-inducible protein (IP-10), monocyte chemoattractant protein-1, macrophage inflammatory protein-3α, and regulated upon activation, normal T cell expressed and secreted (RANTES) (Figure 1). The increase of mRNA expression was observed from 2 to 6 hours before decreasing gradually.

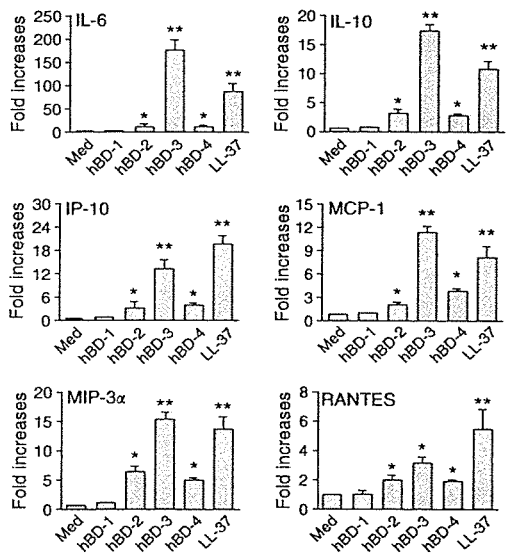

Figure 1. hBDs increase the gene expression of proinflammatory cytokines and chemokines in keratinocytes. Normal human keratinocytes were incubated with 30 μg/ml of hBD-1, -2, -3, -4, and LL-37 or medium alone for 6 hours. Following the incubation, total RNA was extracted, converted into cDNA, and real-time PCR was performed to analyze the changes in gene expression. Each bar shows the mean $\pm$ SD from five separate experiments, each experiment run in triplicate. Values represent fold-increases in gene expression above cells incubated with medium alone (Med). $^*P<0.01$, $^{**}P<0.001$.

Figure 1 shows the data of a 6 hour-stimulation. In contrast to hBD-2, -3, and -4, hBD-1 did not increase the gene expression of above cytokines and chemokines, even at higher concentrations (data not shown). We used 30 μg/ml of each peptide because in preliminary dose-dependent experiments, this concentration induced the maximal mRNA levels of cytokines and chemokines without causing cytotoxicity, as verified by trypan blue exclusion, lactate dehydrogenase (LDH) activity, and cytotoxicity assay using cell-counting kit-8 (CCK-8, data not shown). We also confirmed that another keratinocyte-derived antimicrobial peptide LL-37 significantly induced gene expression of investigated cytokines and chemokines in a similar manner to that seen with hBDs.

hBD-2, -3, and -4 induce the production of cytokines and chemokines by keratinocytes

Because hBDs increase the gene expression of proinflammatory cytokines and chemokines, we postulated that these peptides could also stimulate keratinocytes to produce their respective proteins. After stimulation of keratinocytes with hBDs (30 μg/ml each) for 48 hours, the production of cytokines and chemokines in cell-free supernatants was determined by appropriate ELISA kits. As shown in Figure 2, hBD-2, -3, and -4 induced the production of IL-6, IL-10, IP-10, monocyte chemoattractant protein-1, macrophage inflammatory protein-3α, and RANTES. The cytokine and chemokine production was also dose dependently detectable after stimulation with concentrations of hBDs lower than 30 μg/ml (data not shown). As expected, the effect of hBD-1 on cytokine and chemokine production was not observed. In this respect, hBD-1 used was biologically active because the same reagent has been shown to effectively kill *E. coli* and *Staphylococcus aureus* (Chen *et al.*, 2005). In addition to hBDs, we observed that LL-37 also significantly induced the production of keratinocyte cytokines and chemokines in the same range as hBDs.

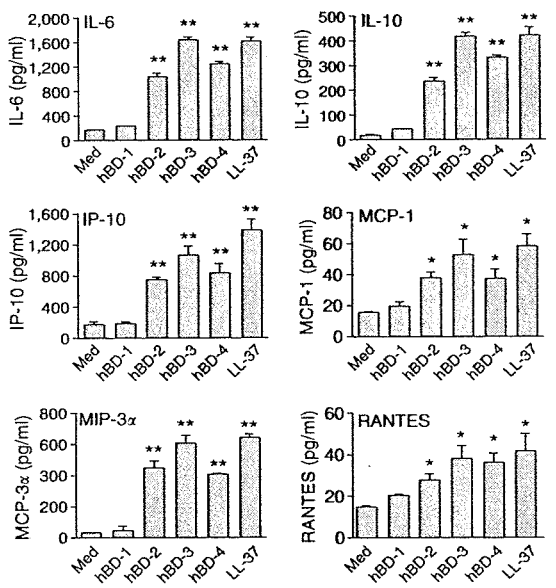

Figure 2. hBDs induce the production of cytokines and chemokines from keratinocytes. Keratinocytes were stimulated with 30 μg/ml of hBD-1, -2, -3, -4, and LL-37 for 48 hours, and the concentrations of different cytokines and chemokines released into the culture supernatants were determined by ELISA. Values are compared between the stimulated and non-stimulated cells (Med: medium alone). $*P<0.05$, $**P<0.01$. Each bar represents the mean ± SD of three to five independent experiments.

Effects of pertussis toxin and U-73122 on hBD-mediated cytokine and chemokine production

It has been reported that hBD-2 chemoattracts T cells and dendritic cells through a G protein receptor CCR6 (Yang *et al.*, 1999) and activates mast cells via unidentified G protein receptors coupled to PLC (Niyonsaba *et al.*, 2001). Thus, to seek whether hBDs activate keratinocytes through G protein- and PLC-mediated signaling pathway, cells were pretreated for 2 hours with 200 ng/ml pertussis toxin (PTx), 10 μM U-73122, or the inactive analog of U-73122, U-73343 before stimulation with 30 μg/ml hBD-1, -2, -3, and -4. PTx and U-73122 pretreatment decreased the stimulatory effects of hBD-2, -3, and -4, as well as LL-37 to elicit the production of IL-6 and IP-10 (Figure 3a and b). Similar results were obtained for IL-10, monocyte chemoattractant protein-1, macrophage inflammatory protein-3α, and RANTES production (data not shown). U-73343 used at the same concentration as U-73122 did not affect hBD- and LL-37-mediated cytokine and chemokine production, demonstrating that the effect of U-73122 was specific. Thus, G protein – PLC

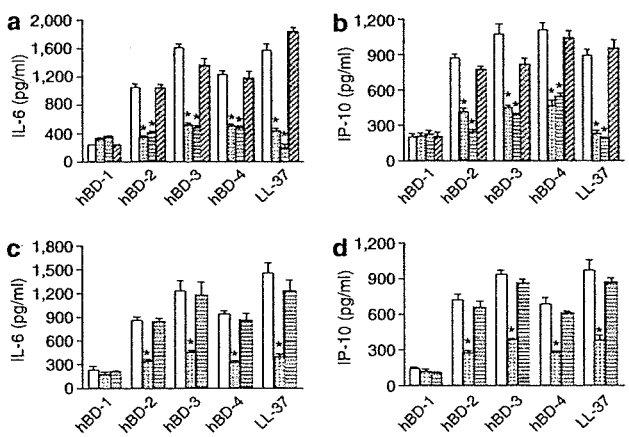

Figure 3. Inhibitory effects of PTx, U-73122, and PLCβ2 siRNA on hBD-induced IL-6 and IP-10 production. (**a** and **b**) Keratinocytes were pretreated with 200 ng/ml PTx (dots), 10 μM U-73122 (horizontal stripes), 10 μM U-73343 (diagonal stripes), or medium alone without inhibitors (open bars) for 2 hours. Cells were then challenged for 48 hours with 30 μg/ml of hBD-1, -2, -3, -4, and LL-37. The concentrations of released IL-6 (a) and IP-10 (b) into the culture supernatants were measured by ELISA. $*P<0.05$. Values are the mean ± SD of three to five separate experiments, and compared between the presence or absence of inhibitors. (**c** and **d**) Keratinocytes were transfected with 100 nM PLCβ2 siRNA (dots) or control-siRNA (horizontal stripes) for 24 hours, cultured overnight in a new medium without supplements, and then stimulated with 30 μg/ml of hBD-1, -2, -3, -4, and LL-37 for 48 hours. ELISA assay was performed as above. $*P<0.05$. Values are the mean ± SD of four separate experiments, and compared between the control cells (open bars) or control-siRNA transfectants.

signaling pathway is required for the activities of hBDs on keratinocytes.

To further confirm the G protein – PLC pathway involvement in hBD stimulatory effects, we attempted to inhibit the downstream of this pathway through knockdown of PLCβ2 by transfecting keratinocytes with PLCβ2 small-interfering RNA (siRNA), because it has been demonstrated that U-73122 inhibits PLCβ2 more potently than other PLCβ isozymes (Hou *et al.*, 2004). Of interest, knockdown of PLCβ2 was associated with a significant reduction of IL-6 and IP-10 production, compared with control cells or control-siRNA transfectants (Figure 3c and d). We further observed that transfection of PLCβ1 siRNA and PLCβ3 siRNA into keratinocytes also moderately reduced IL-6 and IP-10 production (data not shown).

hBDs elicit intracellular Ca^{2+} mobilization by keratinocytes

We next examined the ability of hBDs to mobilize intracellular Ca^{2+} using Fura-2-AM-loaded keratinocytes. In preliminary experiments, the results revealed a dose-dependent stimulatory effect of hBDs, reaching the plateau at 30 μg/ml. As shown in Figure 4, stimulation of keratinocytes with hBD-2, -3, and -4 markedly increased keratinocyte intracellular Ca^{2+} concentration. However, cells challenged with hBD-1 did not show any change in intracellular Ca^{2+} concentration, which was similar to that induced by the control (0.01% acetic acid used as diluent). In same experimental conditions, LL-37 also markedly increased keratinocyte intracellular Ca^{2+} concentration at same levels seen with hBDs.

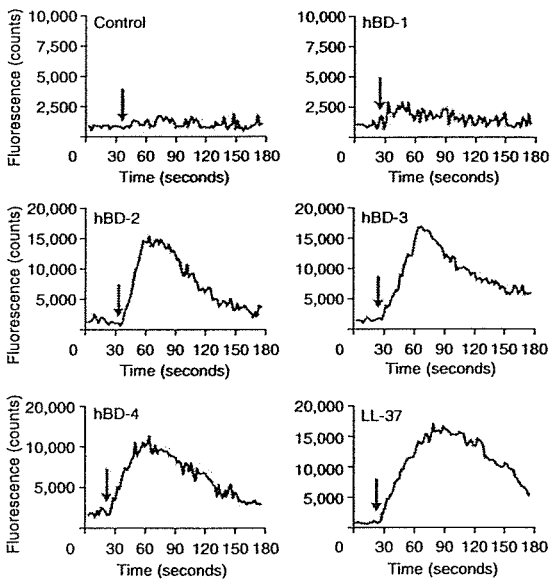

Figure 4. hBDs elicit keratinocyte intracellular Ca^{2+} mobilization. Fura-2-AM-loaded keratinocytes were incubated with 30 μg/ml of hBD-1, -2, -3, -4, and LL-37 or medium containing diluent of 0.01% acetic acid (Control) at 37°C as described in Materials and Methods. Data shown as fluorescence counts are representative of four independent experiments. Arrows indicate the addition of peptides or acetic acid.

hBDs stimulate the migration of human keratinocytes

Because antimicrobial peptides including LL-37 have been reported to mediate migration of airway epithelial cells (Shaykhiev *et al.*, 2005) and keratinocytes (Tokumaru *et al.*, 2005), we hypothesized that hBDs may also stimulate keratinocyte migration. The chemotactic activities of hBDs were analyzed using the Boyden chamber assay. When various concentrations of hBDs (1–40 μg/ml) were added to the lower chambers, keratinocytes into the upper chambers significantly migrated towards hBD-2, -3, and -4, compared to the medium alone. The migratory effect of these peptides was bell-shaped, reaching a peak at 5 μg/ml for hBD-3 and 10 μg/ml for hBD-2 and hBD-4 (Figure 5b, c, and d). There was no increase in migration of cells treated with hBD-1 at all concentrations tested (Figure 5a), or another skin-derived antimicrobial peptide named dermcidin (data not shown), suggesting a specific effect of hBD-2, -3, and -4 on keratinocyte migration. Transforming growth factor (TGF)-α, a well-known keratinocyte chemoattractant was more potent than hBDs (Figure 5e). We observed that a non-coated membrane allowed a slight but significant migration of keratinocytes towards hBDs, however, the migratory effect was markedly enhanced in a collagen-coated membrane. Moreover, there was no significant difference between data

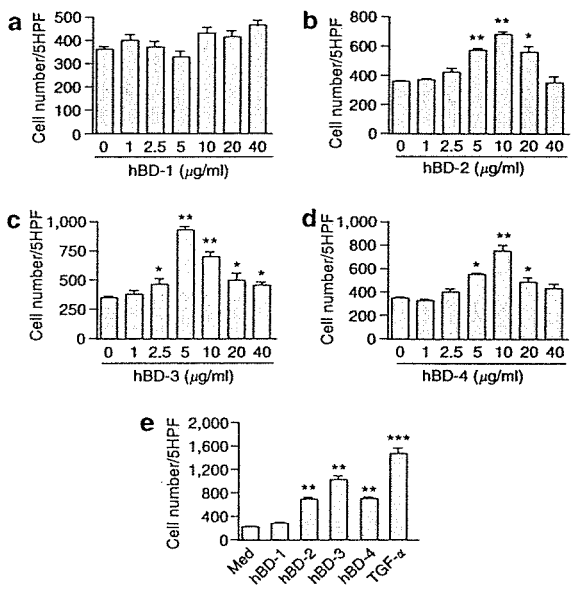

Figure 5. hBDs mediate keratinocyte migration (Boyden chamber assay). The indicated doses (1–40 μg/ml) of (a) hBD-1, (b) hBD -2, (c) hBD -3, and (d) hBD-4 were added to the lower wells, and 5×10^3 cells/well were applied into the upper chambers of 48-well chemotaxis microchamber. Following a 6-hour incubation, the membrane was stained and keratinocyte migration was assessed by counting under a microscope the number of migrated cells through the polycarbonate membrane in five randomly chosen high power fields. Each bar shows the mean±SD of four to six separate experiments. *$P<0.05$, **$P<0.01$ as compared between stimulated and non-stimulated cells. (e) 40 μg/ml hBD-1, 10 μg/ml hBD-2, 5 μg/ml hBD-3, 10 μg/ml hBD-4, and 10 ng/ml TGF-α were used to induce keratinocyte migration as above. **$P<0.01$, ***$P<0.01$ as compared between stimulated and non-stimulated cells.

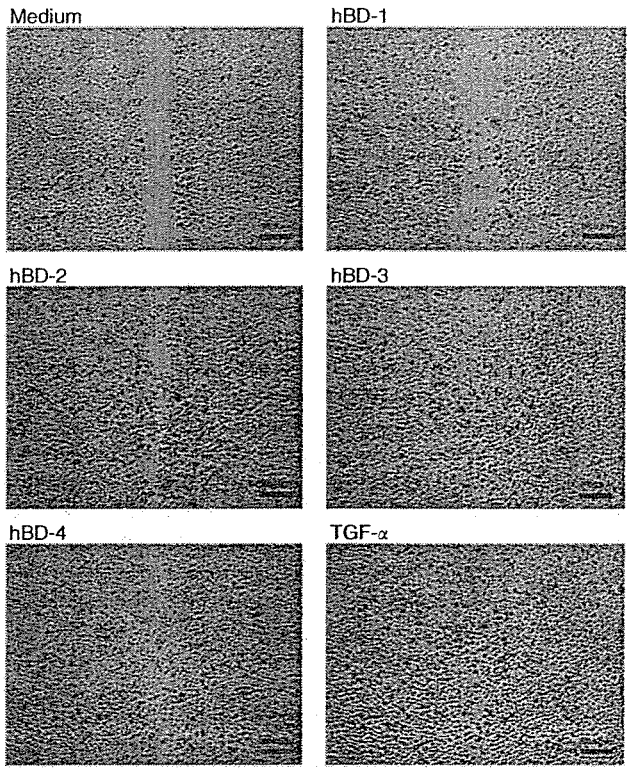

Figure 6. hBDs mediate keratinocyte migration (*in vitro* wound closure assay). A cell-free zone was made in confluent cultures of keratinocytes as described in Materials and Methods. The cells were incubated for 6 hours with 40 μg/ml hBD-1, 10 μg/ml hBD-2, 5 μg/ml hBD-3, 10 μg/ml hBD-4, and 10 ng/ml TGF-α or medium alone (medium) in the presence of mitomycin C. Live cultures were photographed under phase-contrast microscopy. Data shown are representative of three independent experiments. Bar = 200 μm.

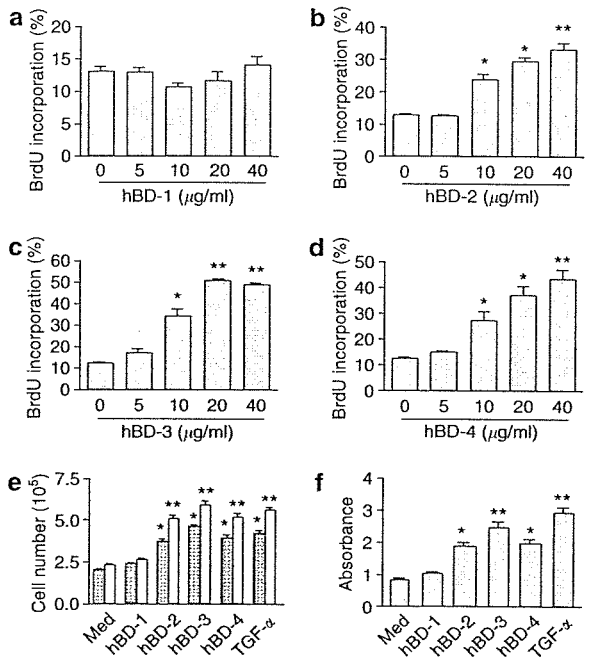

Figure 7. hBDs stimulate human keratinocyte proliferation. Keratinocytes (1×10^4 cells/ml) were cultured on Lab-Tek II eight-chamber glass slides, and subconfluent cells were incubated with 5–40 μg/ml of (**a**) hBD-1, (**b**) hBD -2, (**c**) hBD -3, and (**d**) hBD -4 or medium alone for 48 hours. After incubation with 10 μM BrdU for 1 hour, the numbers of BrdU-positive cells were counted under a light microscope. Data are expressed as a percentage of the BrdU-positive cells (BrdU incorporation). Values are the mean ± SD of five independent experiments. $^*P<0.05$, $^{**}P<0.01$ as compared between stimulated and non-stimulated cells. (**e**) Keratinocytes (1×10^5 cells/ml) were cultured in 12-well plate for 24 hours, followed by stimulation with 40 μg/ml hBD-1, 40 μg/ml hBD-2, 20 μg/ml hBD-3, 40 μg/ml hBD-4, or 100 ng/ml TGF-α for 24 hours (dots) or 48 hours (open bars). Cells were then trypsinized and counted under a light microscope. Values are the mean ± SD of five separate experiments. $^*P<0.05$, $^{**}P<0.01$ as compared between stimulated and non-stimulated cells. (**f**) Keratinocytes (5×10^3 cells/well) were cultured in a 96-well plate and stimulated with 40 μg/ml hBD-1, 40 μg/ml hBD-2, 20 μg/ml hBD-3, 40 μg/ml hBD-4, or 100 ng/ml TGF-α for 48 hours. Cells were treated with 10 μl CCK-8 solution/well and incubated for 3 hours at 37°C. The amount of formazan dye was measured by absorbance at 450 nm with a microplate reader. $^*P<0.05$, $^{**}P<0.01$ as compared between stimulated and non-stimulated cells.

obtained from collagen-, fibronectin-, or vitronectin-coated membranes (data not shown). Thus, one could not exclude haptotactic effect of collagen on hBD-mediated keratinocyte migration.

The Boyden chamber assay data were further complimented by those of *in vitro* wound closure assay. As shown in Figure 6, keratinocytes incubated with optimal doses of hBD-2, -3, and -4 migrated inwardly and covered a greater area of the wound, compared with hBD-1 or medium alone, with TGF-α as a positive control.

hBDs increase keratinocyte proliferation

As LL-37 has been implicated in cell migration and proliferation in epithelial cells, it is probable that hBDs might induce keratinocyte proliferation in addition to migration. Cell proliferation was evaluated by BrdU incorporation complimented with cell count assay and CCK-8 assay. Following a 48-hour incubation, keratinocytes stimulated with 5–40 μg/ml of hBD-2, -3, and -4 dose dependently increased keratinocyte labeling with BrdU (Figure 7b, c, and d). The effect of hBD-1 on enhancing BrdU incorporation was not observed. To confirm BrdU incorporation results, cells were incubated with hBDs and counted over 24 and 48 hours. As shown in Figure 7e, markedly increased cell numbers were observed after stimulation with hBD-2, -3, and -4. Similarly, the CCK-8 assay demonstrated that hBD-2, -3, and -4 enhanced keratinocyte proliferation (Figure 7f).

hBDs induce phosphorylation of EGFR, STAT1, and STAT3

It has been shown that EGFR mediates the migration of keratinocytes, and its activation induces the phosphorylation of both STAT1 and STAT3, which also participate in keratinocyte migration and proliferation (Sano *et al.*, 1999; Kijima *et al.*, 2002; Andl *et al.*, 2004). Furthermore, LL-37 has been recently shown to induce phosphorylation of EGFR and STAT3 (Tokumaru *et al.*, 2005). Thus, we envisaged that hBDs could activate EGFR, STAT1, and STAT3. Following stimulation of keratinocytes with hBDs, the phosphorylation

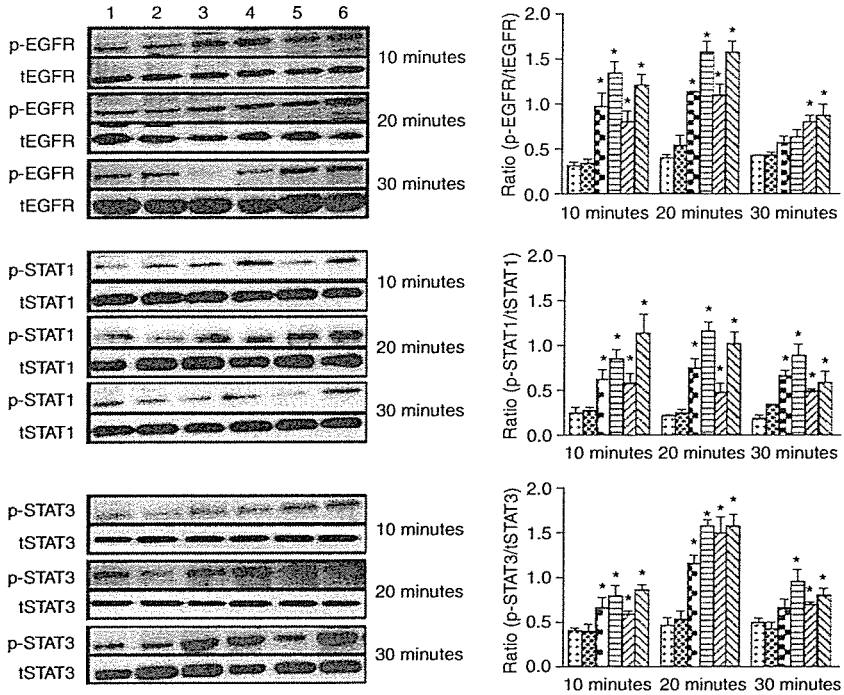

Figure 8. hBDs induce phosphorylation of EGFR, STAT1, and STAT3. Keratinocytes were stimulated with 30 μg/ml of hBD-1, -2, -3, -4, or 5 μg/ml of LL-37 for 10, 20, or 30 minutes, and phosphorylated EGFR (p-EGFR), STAT1 (p-STAT1), or STAT3 (p-STAT3) and total EGFR (tEGFR), STAT1 (tSTAT1), or STAT3 (tSTAT3) levels in cell lysates were determined by Western blot analysis. Lane 1: medium alone, Line 2: hBD-1, Lane 3: hBD-2, Lane 4: hBD-3, Line 5: hBD-4, Line 6: LL-37. Shown is one representative of five independent experiments with similar results. Right panels: Bands were quantified by densitometry using the software program Image Gauge (LAS-1000plus) to allow correction for protein loading. Data represent the ratio of the intensity of phosphorylated protein (p-EGFR, p-STAT1, or p-STAT3) divided by total protein (tEGFR, tSTAT1, or tSTAT3). Values are the mean±SD of five independent experiments. $^*P<0.05$ as compared between stimulated and non-stimulated cells.

of EGFR, STAT1, and STAT3 was analyzed by Western blotting. As observed in Figure 8, hBD-2, -3, and -4 but not hBD-1 induced phosphorylation of EGFR and STAT1 at 10 and 20 minutes, and STAT3 at 20 and 30 minutes. The phosphorylation was quantified by densitometry and shown on right panels of Figure 8.

Activation of EGFR, STAT1, and STAT3 is necessary for hBD-mediated keratinocyte migration and proliferation

To determine whether hBD-mediated EGFR, STAT1, and STAT3 phosphorylation was required for keratinocyte migration and proliferation, cells were pretreated with 20 μg/ml of anti-EGFR antibody, 50 nM of EGFR inhibitor AG 1478, or 100 μM of STAT1 inhibitor fludarabine (Frank *et al.*, 1999), and keratinocyte migration and proliferation assays were subsequently performed as described in Materials and methods. Figure 9 shows that anti-EGFR antibody, AG 1478 and fludarabine markedly reduced hBD-mediated keratinocyte migration (Figure 9a) and proliferation (Figure 9b). Similar effect was observed in LL-37-stimulated keratinocytes. The control IgG antibody did not affect keratinocyte migration and proliferation.

Next, to analyze the role of STAT3 in hBD-induced keratinocyte migration and proliferation, adenovirus-carrying STAT3 dominant-negative mutant (AxCASTAT3F) and the control vector AxLacZ were generated and transfected into keratinocytes (Tokumaru *et al.*, 2005), and cell migration or proliferation was subsequently analyzed. We found that STAT3 dominant-negative significantly suppressed hBD-induced keratinocyte migration and proliferation (Figure 10a and b). Together, these observations imply that the activation of EGFR, STAT1, or STAT3 is required for hBD-mediated human keratinocyte migration and proliferation.

DISCUSSION

The current study demonstrates that endogenous human antimicrobial peptides hBDs stimulate keratinocytes to produce proinflammatory cytokines and chemokines, the production of which is through the G protein and PLC signaling pathway. Furthermore, these peptides mediate keratinocyte migration and proliferation under the control of EGFR, STAT1, and STAT3 activation.

Upon stimulation by antimicrobial peptides, different immune and inflammatory cells have been shown to produce cytokines and/or chemokines. For instance, human neutrophil peptides-1 and -3 stimulate the production of IL-1, -4, -6, tumor necrosis factor-α, and IFN-γ in monocytes (Chaly *et al.*, 2000), and chemokines monocyte chemoattractant protein-1 and macrophage inflammatory protein-2 in lung epithelial cells (Zhang *et al.*, 2001). Moreover, hBDs and LL-37 have been recently reported to enhance the generation of IL-18 in keratinocytes (Niyonsaba *et al.*, 2005). Here we show that

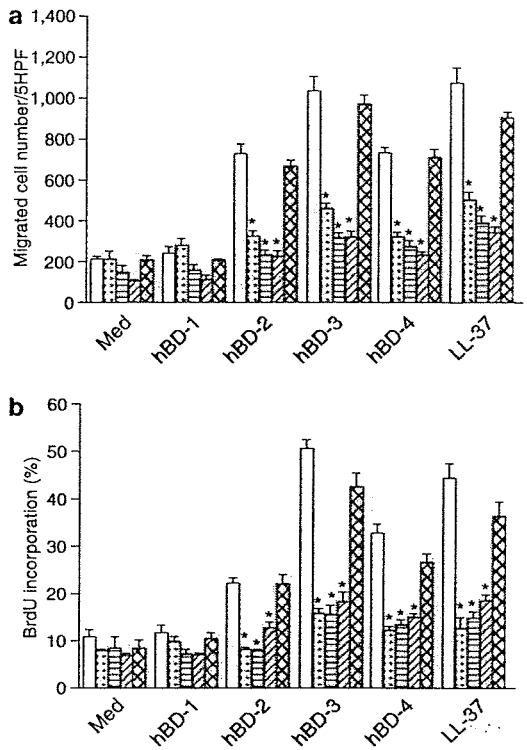

Figure 9. Inhibition of hBD-mediated keratinocyte migration and proliferation by anti-EGFR antibody, AG 1478, and fludarabine. (**a**) 40 μg/ml hBD-1, 10 μg/ml hBD-2, 5 μg/ml hBD-3, 10 μg/ml hBD-4, and 5 μg/ml LL-37 were added to the lower chambers together with 20 μg/ml anti-EGFR antibody (dots), 50 nM AG 1478 (horizontal stripes), 100 μM fludarabine (diagonal stripes), 20 μg/ml control IgG antibody (zigzag lines), or medium alone without inhibitors (open bars) for 6 hours, and the keratinocyte migration was analyzed as described in Figure 5. (**b**) Keratinocytes were pretreated with 20 μg/ml anti-EGFR antibody (dots), 50 nM AG 1478 (horizontal stripes), 100 μM fludarabine (diagonal stripes), 20 μg/ml control IgG antibody (zigzag lines), or medium alone (open bars) for 2 hours, and then stimulated with 40 μg/ml hBD-1, 40 μg/ml hBD-2, 20 μg/ml hBD-3, 40 μg/ml hBD-4, or 20 μg/ml LL-37. Cell proliferation assay was performed as described in Figure 6. $^*P<0.05$ as compared between the presence and absence of inhibitors or antibodies. Values are the mean ± SD of four to six separate experiments.

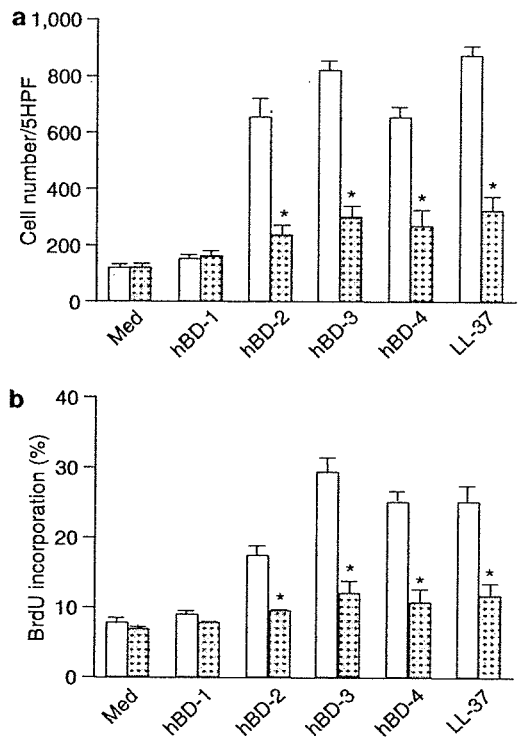

Figure 10. Inhibition of hBD-induced keratinocyte migration and proliferation by STAT3F. (**a**) Keratinocytes were infected with adenoviruses carrying LacZ (AxLacZ) (open bars) or STAT3F (AxCASTAT3F) (dots) at a multiplicity of infection of 1×10^2 plaque-forming units per cell in 1 ml for 24 hours. Cells were then detached, resuspended in culture medium and applied into the upper wells of 48-well chemotaxis microchamber. Thereafter, 40 μg/ml hBD-1, 10 μg/ml hBD-2, 5 μg/ml hBD-3, 10 μg/ml hBD-4, and 5 μg/ml LL-37 were added to the lower chambers. Cell migration was analyzed as described in Materials and Methods section. (**b**) Keratinocytes cultured on Lab-Tek II eight-chamber glass slides were infected with AxLacZ (open bars) or AxCASTAT3F (dots) at a multiplicity of infection of 1×10^2 plaque-forming units per cell in 1 ml for 24 hours. Cells were then incubated with 40 μg/ml hBD-1, 40 μg/ml hBD-2, 20 μg/ml hBD-3, 40 μg/ml hBD-4, and 20 μg/ml LL-37 for 48 hours at 37°C. Cell proliferation assay was performed as described in Materials and Methods. $^*P<0.05$ as compared between AxLacZ- and AxCASTAT3F-infected cells. Values are the mean ± SD of four separate experiments.

hBDs stimulated both the gene and protein expression of various cytokines and chemokines such as IL-6, -10, and IP-10, monocyte chemoattractant protein-1, macrophage inflammatory protein-3α, and RANTES in keratinocytes. In addition, we confirmed that LL-37 had similar stimulatory effects on keratinocytes as seen with hBDs. Therefore, the ability of hBDs and LL-37 to induce the production of proinflammatory cytokines and chemokines suggests the broad role of human antimicrobial peptides in primary immune responses of epidermal cells.

The cytokine and chemokine producing activities of hBDs involved the G protein- and PLC-dependent pathway, as demonstrated by the inhibitory effects of PTx and U-73122 against hBDs, and confirmed by the reduction of cytokine and chemokine production following PLCβ knockdown. Because PTx inhibits $G_{i/o}\alpha$ proteins (Clapham, 1995), and as βγ subunits of G proteins dissociated from $G_{i/o}\alpha$ regulate PLCβ activities (Kehrl, 1998; Knall and Johnson, 1998), it is possible that $G_{i/o}\alpha$ coupled to PLCβ participate in hBD-mediated activation of keratinocytes. Although antimicrobial peptides including hBDs and LL-37 have been shown to function via G protein-coupled receptors, their specific receptors are not yet well known. In our unpublished data, we observed that no cross-desensitization of intracellular Ca^{2+} transients between hBD-1, -2, -3, -4, and LL-37 was detected. Thus, this observation suggests that hBDs and LL-37 act on their target cells through distinct receptors. Further studies will be necessary to identify their functional receptors on keratinocytes.

A multilayered epidermis composed of keratinocytes separates the inner body from the outer environment and protects against microbial pathogens. Hence, keratinocytes are important components of innate immunity, particularly during the wound closure process. In the skin, bacteria and

inflammatory factors as well as wounding are reported to stimulate the production of hBDs by keratinocytes. As the expression of antimicrobial peptides is upregulated at the skin wound site (Dorschner *et al.*, 2001), the current study suggests that hBDs may participate in cutaneous wound closure through their induction of keratinocyte migration and proliferation. The stimulatory effects of hBDs on keratinocyte motility were less strong than those of TGF-α, which is known to induce both keratinocyte migration and proliferation (Cha *et al.*, 1996). Because EGFR, STAT1, and STAT3 are implicated in keratinocyte migration and proliferation (Sano *et al.*, 1999), the effects of hBDs on these molecules were studied. The data demonstrated that hBDs induced phosphorylation of EGFR, STAT1, and STAT3, and that the inhibition of these molecules resulted in suppression of keratinocyte migration and proliferation. Other antimicrobial peptides including α-defensins have been demonstrated to induce the lung epithelial cell proliferation and wound closure (Aarbiou *et al.*, 2002, 2004), and also LL-37 plays a key role in repair of damaged tissue and wound healing by promoting wound neovascularization and re-epithelialization (Heilborn *et al.*, 2003; Koczulla *et al.*, 2003). Thus, human antimicrobial peptides may share properties in activating epithelial surfaces.

Although the concentrations of antimicrobial peptides in human body are not precisely known, it has been proven that the epithelial tissues contain high concentrations of hBDs and LL-37, particularly at sites of infection or inflammation. For example, hBD-2 and LL-37 have been respectively estimated at ~157 μM and ⩾1,605 μM in psoriatic skin lesions (Ong *et al.*, 2002). This shows that the doses of hBDs and LL-37 (ranging from 1 to 40 μg/ml, equivalent to 0.2 to 10 μM) we used in the current report may be adequate for evaluating the physiological roles of hBDs and LL-37 in keratinocytes.

In summary, hBDs induce human keratinocyte migration, proliferation and production of proinflammatory cytokines, and chemokines. Our finding provides evidence that epithelial cell-derived antimicrobial peptides are involved in skin immunity through their activity on keratinocyte production of cytokines and chemokines, migration, and proliferation.

MATERIALS AND METHODS

Reagents

Synthetic hBD-1, hBD-2, hBD-3, and hBD-4 were purchased from Peptide Institute (Osaka, Japan). LL-37 (L^1LGDFFRKSKEKIGKEFKRIVQRIKDFLRNLVPRTES^{37}) was synthesized by the solid-phase method on a peptide synthesizer (model PSSM-8, Shimadzu, Kyoto, Japan). U-73122 (1-[6-([(17β)-3-methoxyestra-1, 3, 5 (10)-trien-17-yl] amino) hexyl]-1H- pyrrole-2.5-dione), U-73343 (1-[6-[(17β)-3-methoxyestra-1, 3, 5 (10)-trien-17-yl] amino] hexyl)-2,5-pyrrolidinedione), PTx, TGF-α, and mitomycin C were purchased from Sigma (St Louis, MO). Fura-2 acetoxy-methylester (Fura-2-AM) was obtained from Dojindo Laboratories (Kumamoto, Japan). Rabbit polyclonal anti-phosphorylated EGFR, STAT1, and STAT3 antibodies and total EGFR, STAT1, and STAT3 antibodies were from Cell Signaling Technology (Beverly, MA). EGFR neutralizing antibody (clone 225) and AG 1478 were purchased from Calbiochem (La Jolla, CA), and fludarabine was from Toronto Research Chemicals (Ontario, Canada).

Keratinocyte culture and stimulation

Normal human epidermal keratinocytes purchased from Kurabo Industries (Osaka, Japan) were cultured in serum-free keratinocyte growth medium, HuMedia-KG2 (Kurabo Industries) containing human epidermal growth factor (0.1 ng/ml), insulin (10 μg/ml), hydrocortisone (0.5 μg/ml), gentamycin (50 μg/ml), amphotericin B (50 ng/ml), and bovine brain pituitary extract (0.4% vol/vol), as reported previously (Niyonsaba *et al.*, 2005). After cells were serially passaged at 60–70% confluence, experiments were conducted with subconfluent cells at passage three or four in the proliferative phase at 60–80% confluence. For stimulation, keratinocytes were cultured in 12-well tissue culture plates, and for total RNA extraction and Western blot, cells were cultured in six-well plates. After removal of growth medium, cells were washed twice with phosphate-buffered saline (PBS) (−) before culture in HuMedia supplemented with only antibiotics for 24 hours. The keratinocytes were subsequently stimulated with hBD-1, -2, -3, and -4 or LL-37 at indicated periods. In some experiments, keratinocytes were pretreated with 200 ng/ml PTx, 10 μM U-73122, or 10 μM U-73343 for 2 hours before stimulation with various peptides.

To quantify the possible cytotoxicity of antibacterial peptides to keratinocytes, LDH activity in the culture supernatants after stimulation was measured using Cytotoxicity Detection Kit – LDH (Roche Diagnostics, Indianapolis, IN) according to the manufacturer's instructions. Percentage of LDH activity in the supernatants was calculated as: ((experimental value–LDH activity released from untreated cells)/(maximum releasable LDH activity in the cells by 1% Triton X-100–LDH activity released from untreated cells)) × 100. Cytotoxicity was also assayed using CCK-8 (Dojindo). Briefly, cells were cultured in a 96-well plate and stimulated with various peptides for 1–48 hours. Cells were then treated with 10 μl CCK-8 solution/well and incubated for 3 hours at 37°C. The amount of formazan dye generated by cellular dehydrogenase activity was measured by absorbance at 450 nm with a microplate reader. Also, trypan blue exclusion was used to determine the cytotoxicity of peptides.

Adenovirus vectors

Dominant-negative mutants of STAT3 (STAT3F) were prepared by substitution of tyrosine 705 with phenylalanine (Tokumaru *et al.*, 2005). Adenovirus vectors encoding STAT3F (AxCASTAT3F) and LacZ (AxLacZ) were generated, purified, and transfected as described previously (Tokumaru *et al.*, 2005). Keratinocytes were infected with adenovirus vectors at a multiplicity of infection of 1×10^2 plaque-forming units per cell in 1 ml of keratinocyte growth medium for 24 hours, and thereafter tested for migration and proliferation.

Total RNA extraction and real-time quantitative PCR

Total RNA was extracted from keratinocytes using Trizol reagent (BRL, Life Technologies, Rockville, MD), according to the manufacturer's instructions. First-strand cDNA was synthesized from 3 μg of total RNA with oligo$(dT)_{12\text{-}18}$ primers using Superscript II RNase H^- reverse transcriptase (Life Technologies), as described before (Niyonsaba *et al.*, 2005). Real-time PCR was performed using the

TaqMan Universal PCR Master Mix (Applied Biosystems, Branchburg, NJ). Amplification and detection of mRNA were analyzed by 7500 real-time PCR System (Applied Biosystems), according to the manufacturer's specifications. All primer/probe sets used in this study were obtained from Applied Biosystems assays on demand. To standardize mRNA concentrations, transcript levels of the housekeeping gene glyceraldehyde-3-phosphate dehydrogenase were determined in parallel for each sample, and relative transcript levels were corrected by normalization based on the glyceraldehyde-3-phosphate dehydrogenase transcript levels. All real-time PCRs were performed in triplicate, and the changes in gene expression were reported as fold-increases relative to untreated controls.

RNA interference

The siRNA duplexes targeting PLC-β1, PLC-β2, and PLC-β3 were purchased from Dharmacon (Chicago, IL). Keratinocytes were plated at a density of 1×10^5 cells/well in six-well plates. Cells were transfected with 100 nM of PLC-β1 siRNA, PLC-β2 siRNA, PLC-β3 siRNA, or control-siRNA as a control using DharmaFECT 1 (Dharmacon) according to the manufacturer's specifications. Gene silencing was conducted for 24 hours, and the efficacy of knockdown was confirmed by real-time PCR analysis. Cells were further cultured overnight in HuMedia without supplements, and subsequently stimulated with various peptides.

ELISA

Cytokines and chemokines released in the cell-free supernatants from non-stimulated or stimulated cultures with 30 μg/ml hBD-1, -2, -3, -4, and LL-37 for 48 hours were measured with ELISA kits from R&D Systems (Minneapolis, MN). Supernatants were stored at −20°C until use for ELISA according to the manufacturer's instructions.

Measurement of intracellular Ca^{2+} concentration

Subconfluent keratinocytes were detached from culture plates using 0.025% trypsin and 0.25 mM EDTA, following two washes with PBS. Cells were then washed twice with PBS containing 0.2% BSA, 0.1% glucose, and 30 μM $CaCl_2$, and resuspended in the same buffer at the density of 2×10^6 cells/ml. After loading with 4 μM Fura-2 AM for 1 hour at 37°C, cells were washed three times, and then resuspended in washing buffer at the concentration of 1×10^6 cells/ml for stimulation. Fura-2-AM-loaded cells were stimulated with 30 μg/ml hBD-1, -2, -3, -4, or LL-37, and fluorescence was measured at 340 and 380 nm excitation and 510 nm emission, using a Hitachi F-4500 spectrofluorometer (Hitachi, Tokyo, Japan).

Cell migration assays

Keratinocyte migration was assayed using a modified Boyden chamber consisting of a 48-well microchamber (Neuro Probe, Gaithersburg, MD). Various concentrations of peptides were added to the lower wells, and an 8-μm pore-size polyvinylpyrrolidone-free polycarbonate membrane (Neuro Probe, Gaithersburg, MD) was placed between the lower wells and upper wells. The membrane was pre-coated with 10 μg/ml type I collagen, 25 μg/ml fibronectin, or 25 μg/ml vitronectin (Sigma) at 37°C for 2 hours, and then washed extensively with PBS. Shortly before the experiment, subconfluent keratinocytes were trypsinized and resuspended in culture medium containing antibiotics only at 1×10^5 cells/ml. A 50-μl aliquot of the cell suspension (5×10^3 cells/well) was placed into the upper wells, then the chamber was incubated for 6 hours at 37°C in a humidified atmosphere of air with 5% CO_2. After incubation, cells adherent to the upper surface of the filter membrane were removed by scraping with a rubber blade. Cells that had migrated through the membrane and adherent to the underside of the filter were fixed with 100% methanol overnight. The filter was then stained with DiffQuick (Kokusai Shiyaku, Kobe, Japan), mounted, and the cell migration was quantified by counting under a light microscope. The results are presented as migrated cell number/five high power fields chosen randomly.

In some experiments, peptides were added to the lower chambers together with PTx (200 ng/ml), U-73122 (10 μM), anti-EGFR antibody (20 μg/ml), AG 1478 (50 nM), fludarabine (100 μM), or control IgG antibody (20 μg/ml), and cell migration towards hBDs was determined as described above. Furthermore, to determine the role of STAT3 in keratinocyte migration, AxCAStat3F, and AxLacZ were transfected into keratinocytes at a multiplicity of infection of 1×10^2 for 24 hours followed by the migration assay.

A second migration assay, the *in vitro* wound closure assay, was performed according to a modified procedure of Li *et al.* (2004). Keratinocytes (1.5×10^5/well) were plated into 12-well culture plate, and after 3 hours of incubation, the confluent monolayer of cells was wounded with a p-200 pipette tip to create a uniform cell-free zone in each well. Cellular debris were removed by PBS washing. Wounded monolayers were then incubated for 6 hours in HuMedia without supplements, containing optimal doses of hBDs. Mitomycin C (10 μg/ml) was always included in the media to prevent cell proliferation. The repopulation of wounded areas was observed under the phase-contrast microscope (Keyence, Osaka, Japan).

Cell proliferation assay

Keratinocytes were cultured at a density of 1×10^4 cells/ml on Lab-Tek II eight-chamber glass slides (Nalge Nunc International, Naperville, IL). Subconfluent cells were incubated with various peptides at indicated concentrations for 48 hours at 37°C. Cell proliferation was evaluated by a BrdU incorporation method using a commercially available BrdU labeling and detection kit II (Roche Diagnostics) according to the manufacturer's instructions, by incubating the peptide-stimulated cells with 10 μM BrdU for 1 hour at 37°C. The percentage of BrdU incorporation was calculated as number of BrdU-positive cells/total number of cells × 100.

Keratinocyte proliferation was further analyzed using CCK-8 according to manufacturer specifications as described above. Moreover, 1×10^5 keratinocytes/well were cultured in 12-well plate for 24 hours, and then stimulated for 24–48 hours with peptides diluted in culture media without supplements. The media was then removed, and cells were washed with PBS, trypsinized, and counted under a light microscope.

The inhibition of keratinocyte proliferation was analyzed by pretreating keratinocytes with PTx (200 ng/ml), U-73122 (10 μM), anti-EGFR antibody (20 μg/ml), AG 1478 (50 nM), fludarabine (100 μM), or control IgG antibody (20 μg/ml) for 2 hours before stimulation with peptides, and the proliferation assay was performed as above by BrdU incorporation method. In parallel experiments, keratinocytes were transfected with adenovirus vectors AxCASTAT3F or AxLacZ followed by stimulation with peptides.